
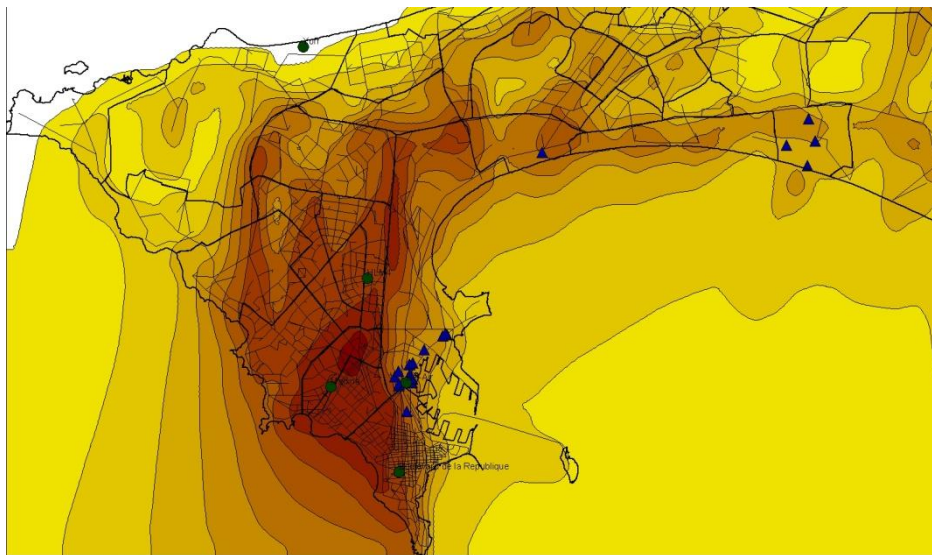


<b>FINANCED BY:</b> Nordic Development Funds	<h2>Project Report</h2>	
<b>Project:</b>	IMPLEMENTATION OF A CENTRAL LABORATORY AND AN AIR QUALITY MONITORING NETWORK IN DAKAR	
<b>Contract:</b>	N°: 003/C/FND/05	

# Preliminary results from air quality modelling in Dakar

Cristina Guerreiro and Vo Thanh Dam



REPORT NO:	6g
CONSULTANTS REFERENCE:	O-105010 OR 52/2010
REV. NO:	Version 1 (July 2010)
NAME OF TASK	Establish and operate the Air quality Management System (AQMS)
ISBN:	978-82-425-2265-8 (Print) 978-82-425-2266-5 (Electronic)

## Table of contents

	Page
<b>Table of contents .....</b>	<b>1</b>
<b>Summary.....</b>	<b>3</b>
<b>1 Introduction.....</b>	<b>5</b>
<b>2 The AirQUIS models .....</b>	<b>5</b>
2.1 The wind field model - MATHEW .....	5
2.2 The dispersion model - EPISODE .....	6
2.2.1 Chemistry model .....	7
2.3 The exposure model .....	7
<b>3 Air quality guidelines and limit values .....</b>	<b>8</b>
<b>4 Input model data .....</b>	<b>9</b>
4.1 Meteorology .....	9
4.2 Model domain and topography data .....	11
4.3 Emission data .....	12
4.4 Population data.....	13
<b>5 Model results .....</b>	<b>15</b>
5.1 NO <sub>2</sub> and NO <sub>x</sub> concentrations.....	15
5.1.1 Background concentrations .....	15
5.1.2 Contribution from all sources.....	16
5.1.3 Contribution from industrial sources.....	19
5.1.4 Contribution from traffic sources .....	22
5.1.5 Contribution from area sources .....	24
5.1.6 Comparison of modelled and measured concentrations.....	27
5.2 SO <sub>2</sub> concentrations .....	28
5.2.1 Background concentrations .....	28
5.2.2 Contribution from all sources.....	29
5.2.3 Contribution from industrial sources.....	30
5.2.4 Contribution from traffic sources .....	31
5.2.5 Contribution from area sources .....	32
5.2.6 Comparison of modelled and measured concentrations.....	32
5.3 CO concentrations.....	34
5.3.1 Background concentrations .....	34
5.3.2 Contribution from traffic and area sources.....	34
5.3.3 Contribution from traffic sources .....	35
5.3.4 Contribution from area sources .....	37
5.3.5 Comparison of model results and measurements .....	38
<b>6 Conclusion .....</b>	<b>40</b>
<b>7 References.....</b>	<b>41</b>





## Summary

Financed by the Nordic Development Fund (NDF), the Norwegian Institute for Air Research (NILU) has supported the Conseil Exécutif des Transports Urbains de Dakar (CETUD) in establishing the Centre de Gestion de la Qualité de l'Air (CGQA) with an Air Quality Monitoring and Management System for Dakar. This project is part of the component entitled as “Amélioration de la qualité de l'air en milieu urbain” (QADAK) of the “Programme d'Amélioration de la Mobilité Urbaine” (PAMU) operated by the Conseil Exécutif des Transports Urbains de Dakar (CETUD).

The current report summarises the preliminary results from air quality modelling in Dakar. The amount of air quality measurement data available at the end of the project was neither adequate nor sufficient to fully test the AirQUIS dispersion model in Dakar. Therefore only a preliminary evaluation of the AirQUIS models and air quality modelling for Dakar was possible to undertake and is presented in the current report.



## 1 Introduction

An air dispersion modelling exercise was carried out for a first evaluation of the impact from the different emission sources in Dakar, Senegal. The modelling is based on the available air emission data and on the available meteorological data from the CGQA monitoring network. The components modelled are NO<sub>2</sub>, NO<sub>x</sub>, SO<sub>2</sub> and CO. Most of the modelling work was undertaken at NILU in February 2010, as part of the on-the-job training of the CGQA modelling expert.

## 2 The AirQUIS models

Air pollution dispersion models are well established and fully implemented parts of the AirQUIS tools. The following modules are part of the main module AirQUIS models:

- Wind field Model, MATHEW (See description in Chapter 2.1);
- Emission Model (See description in Guerreiro and Dam, 2010);
- Dispersion Model, EPISODE (See description in Chapter 2.2);
- Exposure Model (See description in Chapter 2.3).

### 2.1 The wind field model - MATHEW

The MATHEW wind field model is used to calculate three dimensional wind fields for a specified averaging period. The wind-field model implemented in AirQUIS is called CG-MATHEW (Conjugated-Gradient Mass Adjusted Three dimensional Wind field). MATHEW (Sherman, 1978; Foster et al., 1995; Slørdal, 2002) is a diagnostic model designed to produce a gridded three-dimensional mass-conservative mean wind field from time average measured meteorological data. The main characteristics of the wind field model are:

- it incorporates terrain explicitly in order to be site independent;
- it uses available meteorological measurements;
- it is computationally stable;
- it calculates a three-dimensional velocity field with a relatively large number of grid points in a relative short computer time.

MATHEW generates mass consistent wind fields by minimal adjustment of input fields derived from observations. The adjustments are performed by a constrained variational minimisation using finite-difference methods and a conjugate gradient solution. The requirement of minimal adjustment maintains consistency with available meteorological measurements, while the use of observed atmospheric

stability parameters govern the relative amounts of change in the vertical and horizontal wind components.

The calculation grid used in the AirQUIS version of MATHEW is a terrain following sigma co-ordinate system. This means that the lowest level of the model follows the terrain and the highest level is a flat plane. The vertical sigma co-ordinates are thus defined as:

$$\sigma(x, y, z) = H_0 \frac{z - h(x, y)}{H_0 - h(x, y)} \quad (1)$$

where  $H_0$  is the height of the uppermost grid level,  $z$  is the elevation and  $h$  is the terrain height. The velocity components are defined on staggered grid faces so that the mass-consistency constraint is cell-flux, rather than grid point, based.

## 2.2 The dispersion model - EPISODE

The air dispersion model implemented in AirQUIS is called EPISODE. It is a combined 3D Eulerian/Lagrangian air pollution dispersion model for urban and local-to-regional scale applications (Slørdahl et al., 2003). The model may be used to calculate air pollution in an area with several simultaneous emission sources such as road traffic (line sources), domestic or home heating (area sources) and individual industry sources (point sources). The model produces ground level hourly or half hourly average concentrations as gridded data and/or at individually placed receptor points. Since the output from the model consists of hourly or half hourly data, the results may also be used to calculate various statistical values such as maximums, averages, and percentiles.

The EPISODE model itself consists of:

- a Eulerian grid model, in which advection and dispersion on a predefined grid is carried out for field and area sources.
- two different Gaussian-dispersion models for point source dispersion calculations. These are a puff/trajectory model (INPUFF) and a segmented plume/trajectory model.
- a Gaussian-plume line source model (HIWAY-2) for sub-grid traffic dispersion calculations.
- a chemistry model for the reactive species  $O_3$ , NO and  $NO_2$ . A photo-stationary state is assumed.

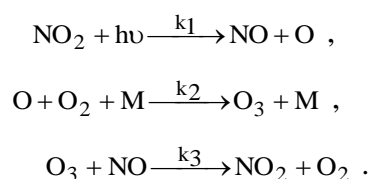
The Gaussian dispersion models used for point and line sources are known as sub-grid models as they can be used on scales less than the defined grid.

For a more detailed description of the EPISODE dispersion model see Denby (2008) and Slørdal et al., (2003).

### 2.2.1 Chemistry model

All compounds simulated within EPISODE are treated as non-reactive species with the exception of NO, NO<sub>2</sub> and O<sub>3</sub>. For the dispersion and transport calculations these components are also treated as non-reactive but at the end of every hour the photo stationery state assumption is applied and the concentration of these components is calculated accordingly.

The photo stationery state is the instantaneous equilibrium between the following three reactions:



The steady-state assumption implies that NO<sub>x</sub> (the sum of nitrogen oxides) and O<sub>x</sub> (oxidants) are conserved, where NO<sub>x</sub> and O<sub>x</sub> are defined as:

$$[\text{NO}_x] = [\text{NO}] + [\text{NO}_2] , \quad \text{and} \quad [\text{O}_x] = [\text{O}_3] + [\text{NO}_2] .$$

By these assumptions the three components NO, NO<sub>2</sub> and O<sub>3</sub> can be found by the solution of a second-degree equation in O<sub>3</sub>.

This is a valid assumption in urban areas at a short distance away from the emissions when net ozone formation is not significant. In polluted areas in the north in winter this will be a good assumption. However, when the solar UV-radiation is stronger, either because of a more southern location or in summer, net ozone formation can take place in urban areas a certain distance away from the main emission sources. Then the assumption of conservation of O<sub>x</sub> and NO<sub>x</sub> is not valid and a more detailed chemical description is needed.

### 2.3 The exposure model

AirQUIS includes a model for estimating the population exposure to air pollution. Air pollution impact on health can be estimated by combining calculated concentrations, either in grid or building addresses, and the population distribution. Exposure estimates can be used to describe how many people are exposed to air pollution above air quality guidelines.

Based on dispersion calculations, the exposure estimations may be performed by combining the concentrations with population data either in field or in building points. For a more detailed description of the exposure model see the Denby (2008).



### 3 Air quality guidelines and limit values

The modelled results should be compared to the air quality guidelines and standards. In this chapter we present the World Health Organisation guidelines and the Senegalese air quality limit values.

The Senegalese Norm NS 05-062 (2003) specifies limit values for ambient air pollution concentration, adopted in 2001. Table 1 presents a summary of these limit values, compared to World Health Organisation (WHO, 2000; WHO, 2005) air quality guidelines. It is important to note that the PM<sub>10</sub> maximum allowed limit value in Senegal is very high compared to the WHO guidelines and other international standards. Table 2 presents the existing and proposed air quality limit values for Senegal, as described in the report Air quality standards for Senegal (Sivertsen et al, 2010a).

Table 1: Existing Senegalese air quality limit values compared to the 2005 WHO guidelines, expressed in  $\mu\text{g}/\text{m}^3$ .

Pollutant	Averaging time	Maximum Limit Value	
		WHO	Senegal
Sulphur Dioxide (SO <sub>2</sub> )	1 hour	500 (10 min)	-
	24 hours	50 *	125
	Year	-	50
Nitrogen Dioxide (NO <sub>2</sub> )	1 hour	200	200
	Year	40-50	40
Ozone (O <sub>3</sub> )	1 hour	150-200	-
	8 hours	120	120
Carbon Monoxide (CO)	1 hour	30 000	-
	8 hours	10 000	30 000 (24h)
Particles <10 $\mu\text{m}$ (PM <sub>10</sub> )	24 hours	50 *	260
	Year	20 *	80
Lead (Pb)	Year	0.5-1.0	2

\*Interim target

Table 2: Existing and proposed Senegalese air quality limit values, expressed in  $\mu\text{g}/\text{m}^3$ .

Pollutant	Averaging time	Maximum Limit Value in Senegal	
		Existent	Proposed
Sulphur Dioxide ( $\text{SO}_2$ )	1 hour	-	-
	24 hours	125	125
	Year	50	50
Nitrogen Dioxide ( $\text{NO}_2$ )	1 hour	200	200
	Year	40	40
Ozone ( $\text{O}_3$ )	1 hour	-	-
	8 hours	120	120
Carbon Monoxide ( $\text{CO}$ )	1 hour	-	30 000
	8 hours	30 000 (24h)	10 000 (8 h)
Benzene ( $\text{C}_6\text{H}_6$ )	Year	-	5
Particles <10 $\mu\text{m}$ ( $\text{PM}_{10}$ )	24 hours	260	150
	Year	80	50
Particles <2,5 $\mu\text{m}$ ( $\text{PM}_{2,5}$ )	24 hours	-	50
	Year	-	25
Lead (Pb)	Year	2	2

\*Interim target

## 4 Input model data

### 4.1 Meteorology

The hourly meteorological data measured by the CGQA monitoring network and available for Dakar was used for the preliminary air quality modeling exercise. After the first quality control of the available monitoring data in February (at the time the modelling work was done), only January data had satisfactory quality and could be used as input to the dispersion model. The modelled period was therefore restricted to the period from 01.01.2010 to 31.01.2010. The meteorological parameters used as an input to the windfield model, MATHEW, are: Temperature measured at two different heights, wind speed and wind direction.

The wind rose for the modelled period (i.e. from 01.01.2010 to 31.01.2010) is given in Figure 1 for the meteorological station of the CGQA monitoring network located at HLM4.

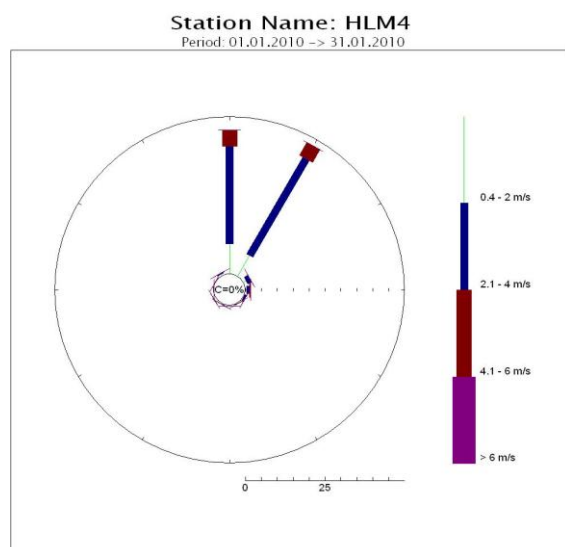


Figure 1: Wind rose for HLM4 station, January 2010

The prevailing winds in January 2010 were from north to north-northeast (Figure 1), which is normal for this time of the year. The wind speed was on average 2,9 m/s and the maximum was 6,2 m/s.

Figure 2 shows that the highest average wind speed occurred when the wind was blowing from the sectors north (360°) and north-northeast (30°).

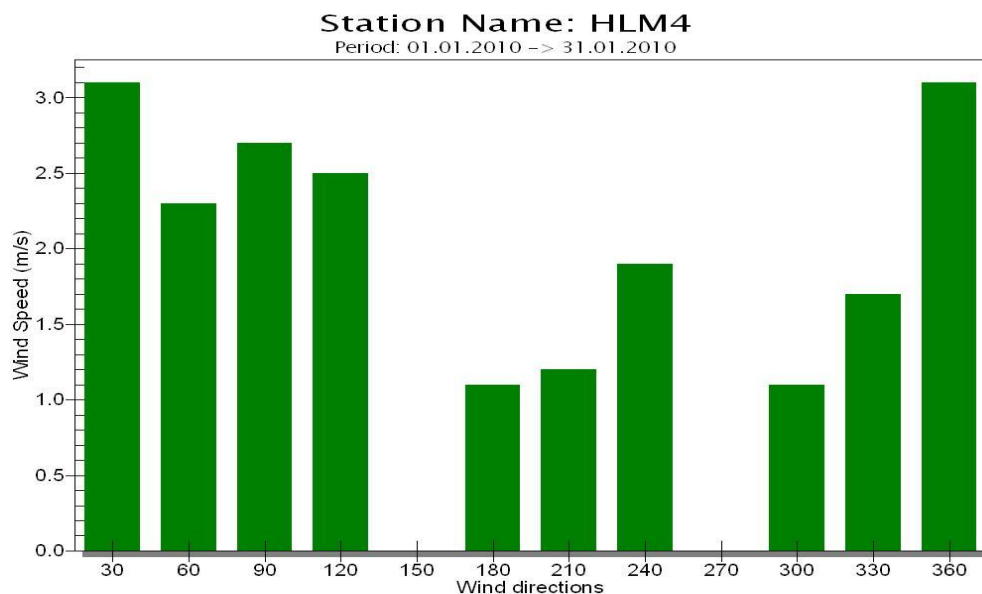


Figure 2: Average wind speed for each of twelve 30-degree sectors.

The average wind speed when it was blowing from northerly directions was about 3 m/s, while from southerly direction it was between 1 and 1,7 m/s.

The atmosphere stability is estimated as the difference of the temperatures measured at 10 meters and 2 meters of height (DT), which was estimated at the

meteorological tower station HLM4. Stability classes were established and defined as “stable atmosphere” ( $DT > 0.3^{\circ}\text{C}$ ), “light stability” ( $0^{\circ}\text{C} < DT < 0.3^{\circ}\text{C}$ ), “neutral” ( $-0.3^{\circ}\text{C} < DT < 0^{\circ}\text{C}$ ) and “unstable atmosphere” ( $DT < -0.3^{\circ}\text{C}$ ). The results indicate that stable conditions occurred during night time, whereas the daytime condition was mostly unstable (Figure 3).

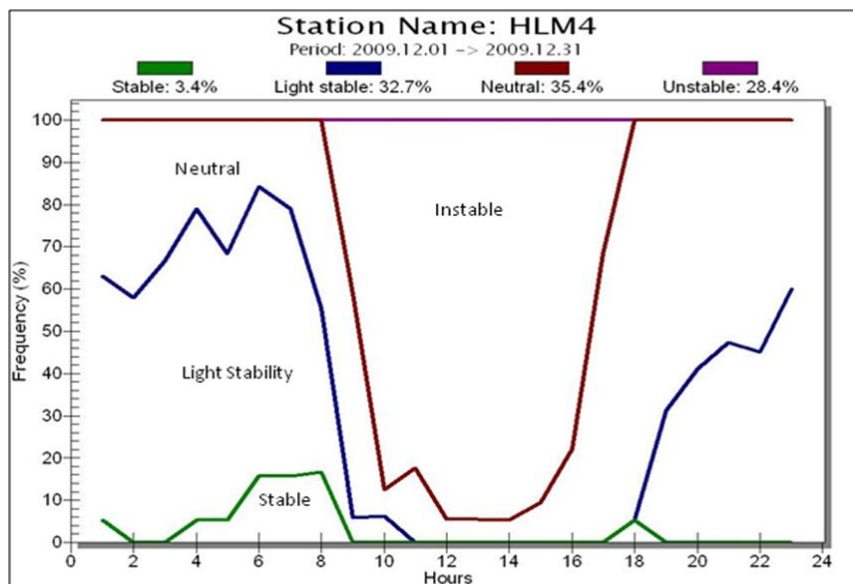


Figure 3: Stability conditions measured at the meteorological station HLM4 (Dakar, January 2010).

The maximum and minimum temperatures measured in January 2010 were 36,3 and 15,8 °C, respectively (Table 3). The average value was 23,5 °C. The highest daily average temperature of 36,3 °C occurred on Monday 16 January at 14:00 hours.

Table 3: Temperature, humidity and pressure measured at HLM4 January 2010.

Parameters	AVERAGE	MIN	TIME FOR MIN	MAX	TIME FOR MAX
Temperature	23.5	15.8	2010.01.08 22:00	36.3	2010.01.16 14:00
Relative Humidity	61.9	11	2010.01.14 15:00	97	2010.01.01 08:00
Pressure	1008.9	961	2010.01.19 14:00	1013	2010.01.11 23:00

#### 4.2 Model domain and topography data

The topographic data for Dakar is presented in Figure 4 with the modelled domain chosen for the air pollutant dispersion calculations. The domain has 30 km in the direction west-east and 17 km in the direction south-north. The concentrations are calculated for each grid cell with a resolution of 500 x 500 m<sup>2</sup>. In total the domain has 60 x 34 = 2040 grid cells.

The more grid cells the modelled domain has and the more emission sources the model has to calculate for, the more computational (CPU) expensive the runs become. The presented domain and resolution was an optimal choice for modelling the greater Dakar region. For modelling exercises where a finer resolution is required, the domain will have to be reduced. On the other hand, if modelling for a greater domain is desirable and the necessary input data is available, the domain may be extended and resolution decreased.

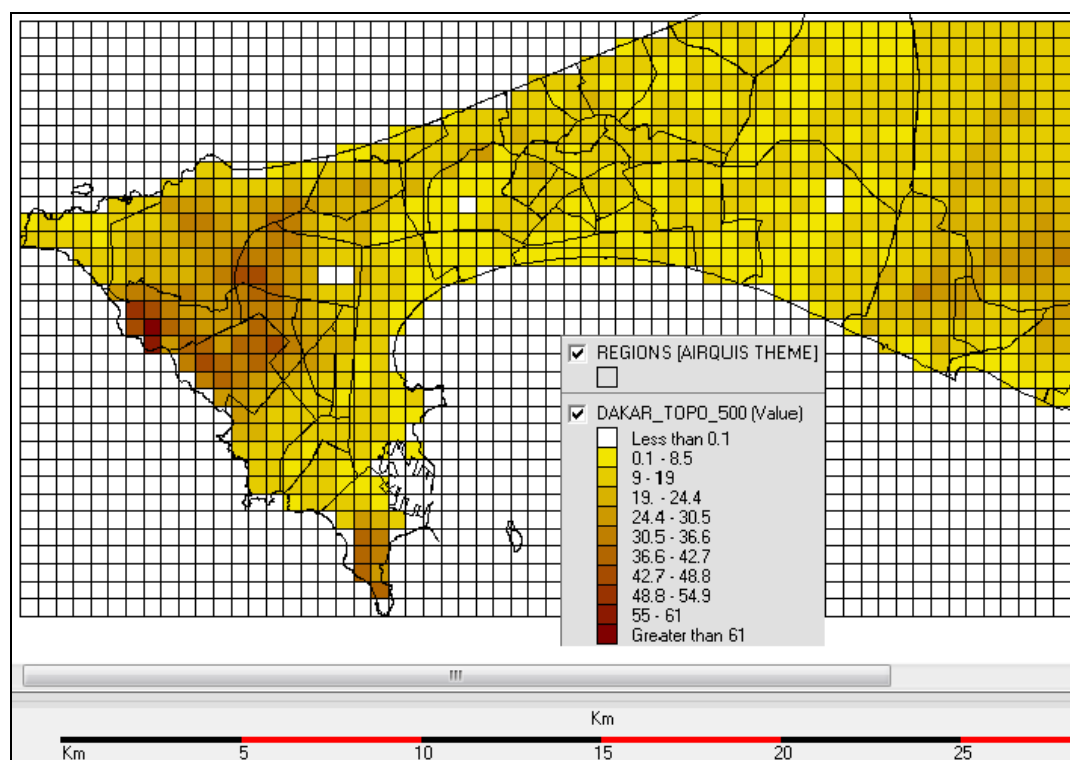


Figure 4: Topographic data for Dakar and modelled domain. Altitude given in meters above sea level.

### 4.3 Emission data

The emission data used as input to the dispersion model is the available data in the AirQUIS emissions database for Dakar, as described in Guerreiro and Dam (2010).

The data in the emission inventory is divided into three types of sources:

Point sources – Industrial emissions, emitted through stacks;

Line sources – Vehicle emissions from road transport;

Area sources - Diffuse sources of pollution. In the inventory they include emissions from charcoal and wood burning in households in Dakar

Table 4 shows the total emissions by source type for all the sources included in the AirQUIS emission database and for the components modelled, whereas the relative contribution from each type of source to the total emissions is shown in Table 5. NO<sub>x</sub>, NO<sub>2</sub>, SO<sub>2</sub> and CO were chosen as the components for the preliminary dispersion modelling exercise, as there is enough emission data to model a representative concentration field.

Table 4: Total emissions by source type for the sources included in the AirQUIS emission database for the modelled components.

Source	Emission (tonnes/year)			
	NO <sub>x</sub>	NO <sub>2</sub>	SO <sub>2</sub>	CO
Industry	4291	218	9859	49*
Traffic	8920	1025	1030	51263
Area	115	11.5	105	98057
<b>Total</b>	<b>13326</b>	<b>1254</b>	<b>10994</b>	<b>149369</b>

(\*) Data from 2 of 15 main industries in Dakar, missing data for the others.  
Not included in the modelled

Table 5: Relative contribution from source type to the total emission in the inventory for the modelled components.

Source	Percentage of total emission (%)			
	NO <sub>x</sub>	NO <sub>2</sub>	SO <sub>2</sub>	CO
Industry	32	17	90	*
Traffic	67	82	9	34
Area	1	1	1	66

(\*) Data from 2 of 15 main industries in Dakar, missing data for the others. Not included

#### 4.4 Population data

Population data was converted from the available population data for the “communes d’arrondissement” to the grid cells of the model domain. This means that the population data were converted from the regions (polygons) values into grid cell (field) values, as part of the preparation of the dispersion model input data (Equation 2).. For instance the population calculated in region A was distributed between all the grid cells that are in contact with region A (marked with • in Figure 5), according to:

$$\text{Value in Grid cell} = \frac{\text{Total emission in region A} \times \text{Area of grid cell inside region A}}{\text{Area of region A}} \quad (2)$$

It is assumed that the population is homogeneous distributed within each “commune d’arrondissement”. Figure 6 shows the population distribution for Dakar on the model grid.

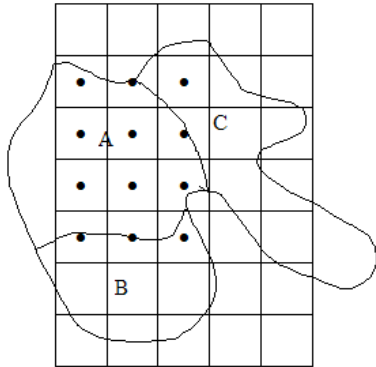


Figure 5: The population in a region is converted into model grid cell values. A, B and C are different regions.

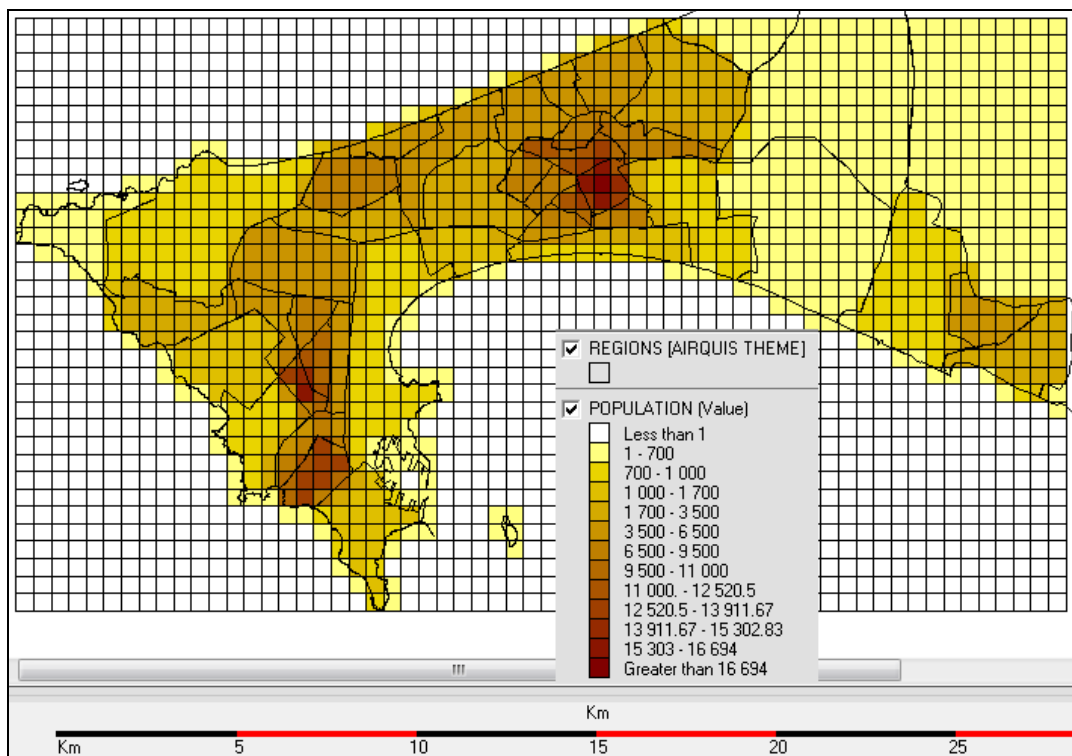


Figure 6: Population distribution for Dakar on the model grid. Unit: Number of people in each grid cell of 500 m x 500 m.

## 5 Model results

The results from the dispersion modelling of air pollutants from the industry, traffic and area sources in Dakar are presented in this chapter. The results show the contributions from each source type to the ground level ambient concentrations of the air pollutants when sufficient emission data is available to allow trustworthy calculations. The total concentrations modelled for all sources are also presented.

The model has calculated hourly concentrations for the period from 01.01.2010 to 31.01.2010 on a 1 km x 1 km resolution grid and at some monitoring stations location, for a first attempt to compare modelled and measured concentrations.

The modelling period had to be restricted to one month (i.e. January 2010), as the CGQA monitoring network has been operating for a short period of time and the measurements from January (2010) are the only ones that provides data of reliable quality.

### 5.1 NO<sub>2</sub> and NO<sub>x</sub> concentrations

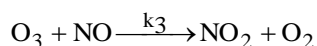
#### 5.1.1 Background concentrations

##### NO<sub>2</sub> and NO<sub>x</sub> background concentrations

To simplify the interpretation of the modelled concentration results and the contribution from the different source types to the ambient air concentrations, a background concentration of 0 µg/m<sup>3</sup> for NO<sub>2</sub> and NO<sub>x</sub> were assumed. Even though the measured average background concentration of NO<sub>2</sub> in January 2010 was 4 µg/m<sup>3</sup> and of NO<sub>x</sub> was 6 µg/m<sup>3</sup> (Sivertsen et al, 2010b).

##### O<sub>3</sub> background concentration

For the NO<sub>2</sub> model calculations, regional background ozone (O<sub>3</sub>) hourly concentrations are needed as an input to the model, for the calculation of the NO<sub>2</sub> formed by the oxidation reaction that transforms the emitted NO into NO<sub>2</sub> concentrations, as given in the equation below:



measured at the regional background monitoring station Yoff were used. When O<sub>3</sub> concentration data was not available, a default value of 40 µg/m<sup>3</sup> was used. The measured concentrations are presented in the report "Air Quality Monitoring in Dakar - Monthly Report N° 01/2010" (Sivertsen et al, 2010b).

Note that the measured concentrations of O<sub>3</sub> at Yoff were lower than expected. This assumption was proved correct after an O<sub>3</sub> measurement campaign using passive diffusion samplers was carried out. The results showed an average O<sub>3</sub> concentration of 49 µg/m<sup>3</sup> by passive diffusion samplers and an average O<sub>3</sub> concentration of 30 µg/m<sup>3</sup> measured by the average O<sub>3</sub>-monitor at the Yoff



monitoring station. The measurement period of the comparison campaign was from 03.03.2010 to 18.03.2010.

This means that the  $O_3$  background concentrations used in the modelling exercise are lower than the real background  $O_3$  levels and that the modelled  $NO_2$  concentrations may be underestimated, due to an unreal limitation of available  $O_3$ . For a more detailed description of the chemistry model, see Chapter 2.2.1.

### 5.1.2 Contribution from all sources

Average and hourly maximum concentration fields were calculated for  $NO_2$  and  $NO_x$ , taking into account the emissions from all sources included in the AirQUIS emission database (Guerreiro and Dam, 2010).

The average concentration fields of  $NO_x$  and  $NO_2$  calculated with emissions from all sources are shown in Figure 7 and

Figure 8, respectively. The maximum  $500 \times 500 \text{ m}^2$  average modelled concentration is  $34 \mu\text{g}/\text{m}^3$  for  $NO_2$  and  $83 \mu\text{g}/\text{m}^3$  for  $NO_x$ . In order to account for the  $NO_2$  concentration transported from outside the model domain, the regional background concentration of  $NO_2$  of  $4 \mu\text{g}/\text{m}^3$  (see Chapter 5.1.1) should be added to the modelled concentrations, leading to an average  $NO_2$  concentration of  $38 \mu\text{g}/\text{m}^3$ . This is a quite high concentration of  $NO_2$ , considering that not all sources have yet been included in the emission inventory (See gap analysis chapters in Guerreiro and Dam (2010)). In addition,  $NO_2$  average concentration is comparable to the Senegalese yearly average limit value of  $NO_2$  (i.e.  $40 \mu\text{g}/\text{m}^3$ ).

The hourly maximum concentration fields of  $NO_x$  and  $NO_2$  calculated with emissions from all sources are shown in Figure 9 and Figure 10, respectively. The model chooses the hour with the highest calculated concentration within the modelled period (i.e. January 2010) for each grid cell, and attributes it to the grid cell as the maximum hourly concentration. This means that the values at different grid cells represent concentrations modelled for different hours. The maximum  $500 \times 500 \text{ m}^2$  hourly concentration is  $133 \mu\text{g}/\text{m}^3$  for  $NO_2$  and  $847 \mu\text{g}/\text{m}^3$  for  $NO_x$ . The Senegalese limit value for hourly  $NO_2$  concentrations is  $200 \mu\text{g}/\text{m}^3$ . Note that the modelled results presented here represent concentrations averaged within a grid cell of  $500 \times 500 \text{ m}$ . The concentrations of  $NO_2$  near on the road side may be higher.

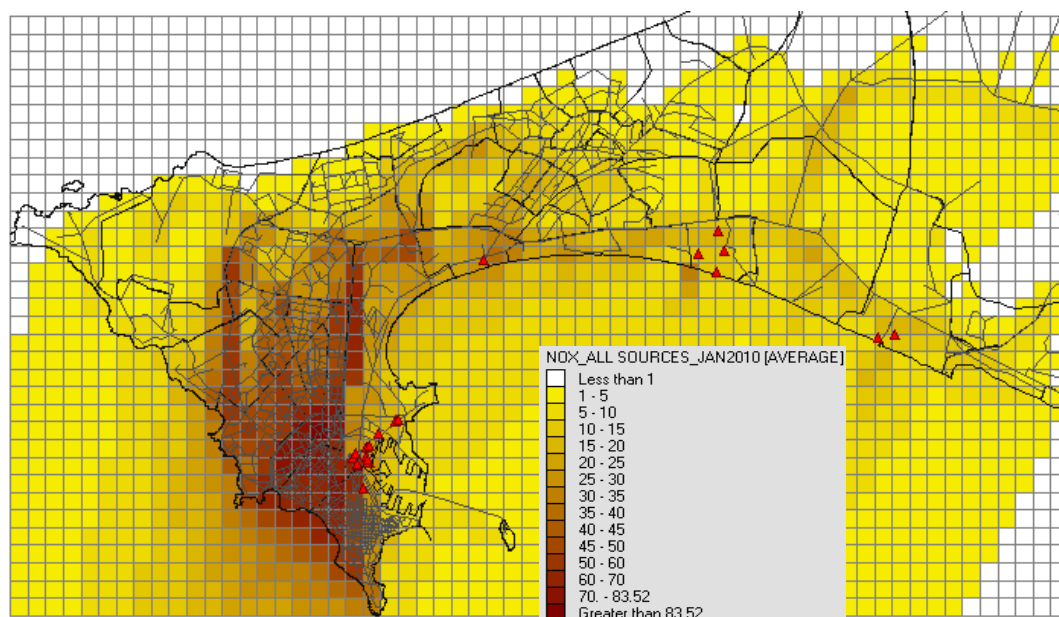


Figure 7: Average concentration of NO<sub>x</sub> for January 2010, modelled with emissions from all sources. The red triangles in the figures indicate the location of the industrial stacks.

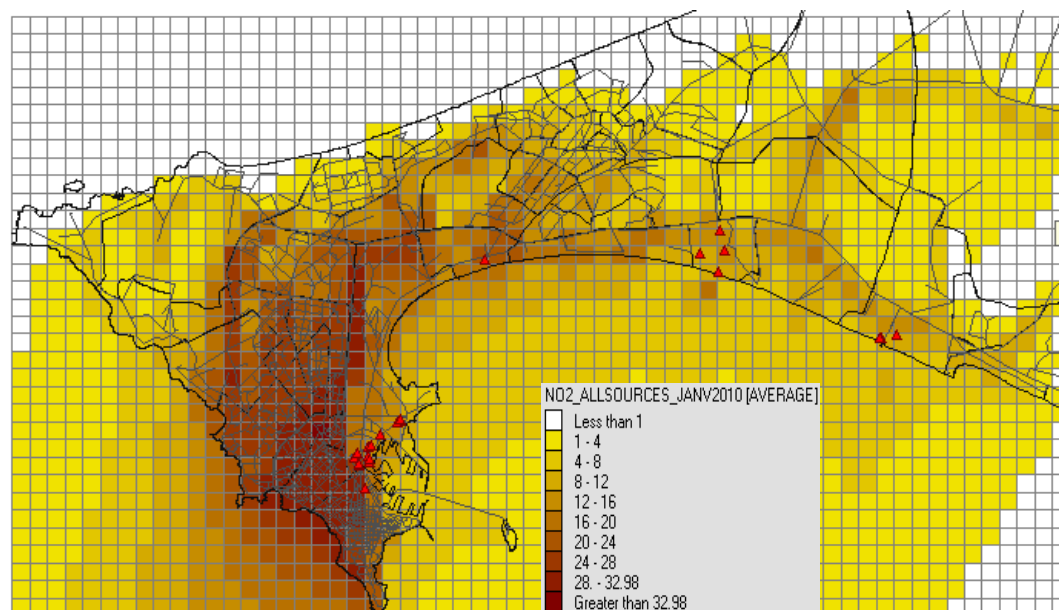


Figure 8: Average concentration of NO<sub>2</sub> for January 2010, modelled with emissions from all sources.

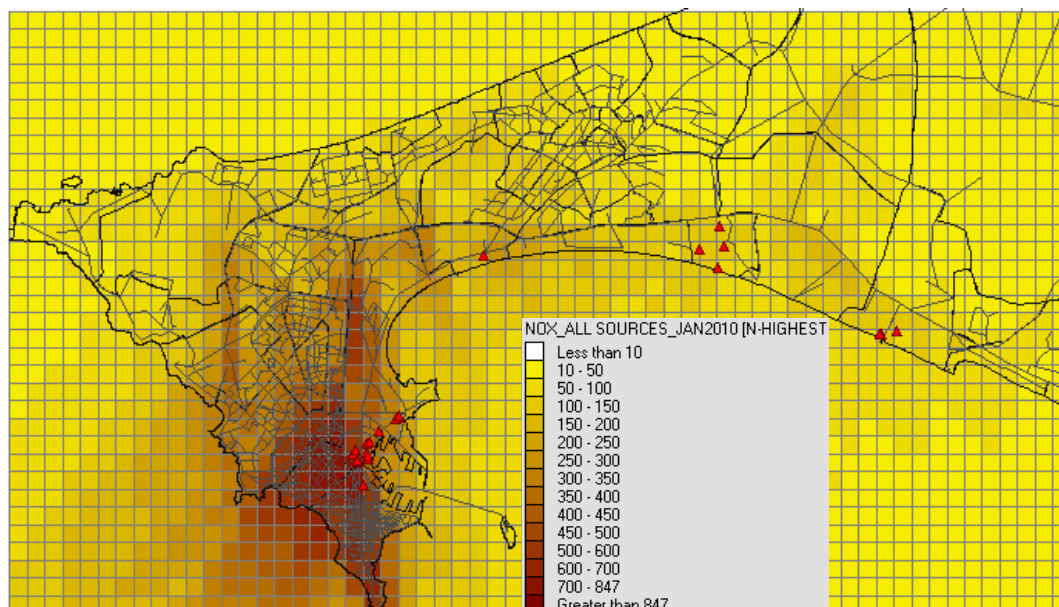


Figure 9: Maximum hourly concentration of NO<sub>x</sub> in January 2010, modelled with emissions from all sources.

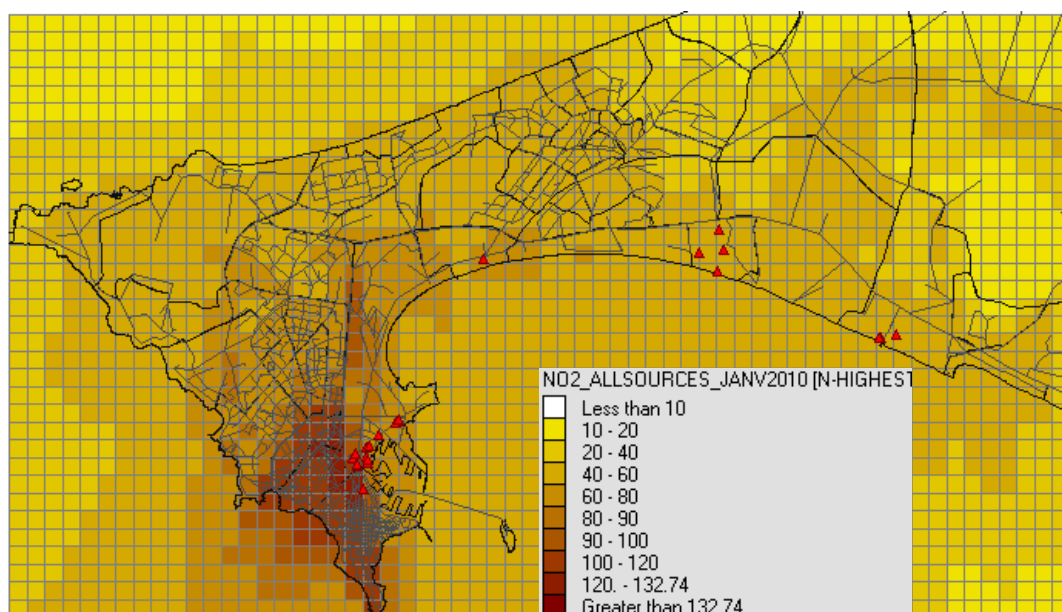


Figure 10: Maximum hourly concentration of NO<sub>2</sub> in January 2010, modelled with emissions from all sources.

### 5.1.3 Contribution from industrial sources

The average concentration fields of  $\text{NO}_x$  and  $\text{NO}_2$  calculated with emissions from industrial sources included in the AirQUIS emission database (Guerreiro and Dam, 2010) are shown in Figure 11 and Figure 12 and

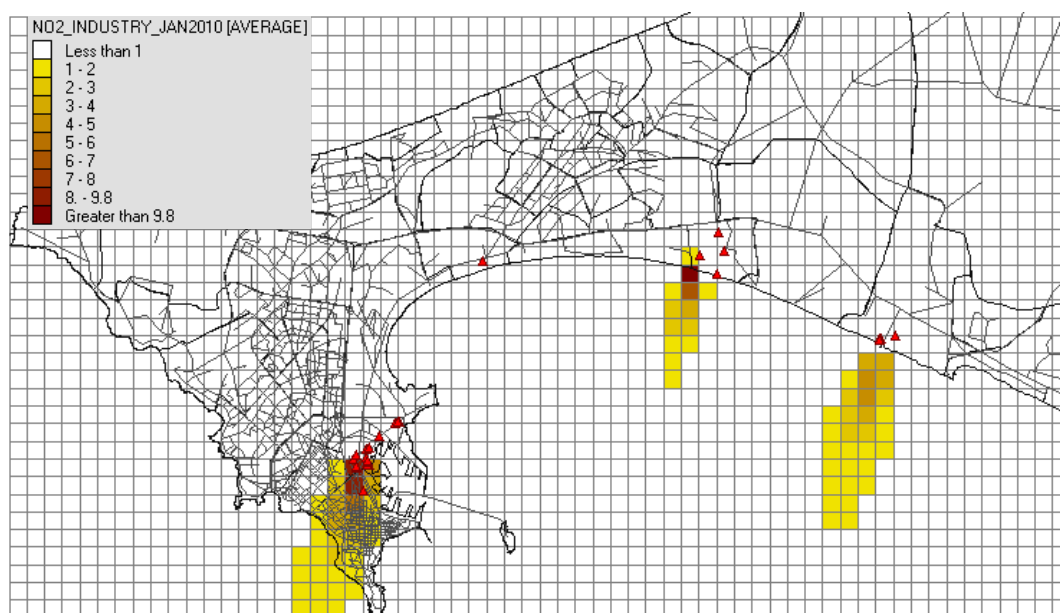


Figure 12, respectively. The maximum  $500 \times 500 \text{ m}^2$  average modelled concentration is  $10 \mu\text{g}/\text{m}^3$  for  $\text{NO}_2$  and  $22 \mu\text{g}/\text{m}^3$  for  $\text{NO}_x$ .

The hourly maximum concentration fields of  $\text{NO}_x$  and  $\text{NO}_2$  calculated with emissions from industrial sources are shown in Figure 13 and Figure 14, respectively. The maximum  $500 \times 500 \text{ m}^2$  hourly concentration is  $41 \mu\text{g}/\text{m}^3$  for  $\text{NO}_2$  and  $101 \mu\text{g}/\text{m}^3$  for  $\text{NO}_x$ . Note that the model chooses the hour with the highest calculated concentration within the modelled period (January 2010) for each grid cell, and attributes it to the grid cell as the maximum hourly concentration. This means that the values at different grid cells represent concentrations modelled for different hours.

In average the industrial sources included in the emission database contribute to about 4% of the  $\text{NO}_2$  concentrations calculated with the contribution from all sources. This is despite the fact that the industrial sources contribute to 32% of the total  $\text{NO}_x$  emissions and to 17% of the primary  $\text{NO}_2$  emissions (Table 5). The reason for this is that the industrial emissions are emitted through stacks, up to 76 meters high. The emitted plume is normally elevated by the exit velocity and high temperature of the exhaust gas and disperses higher in the air before meeting the ground, while traffic emissions are emitted at ground level and area sources at about 3 to 4 meters height.

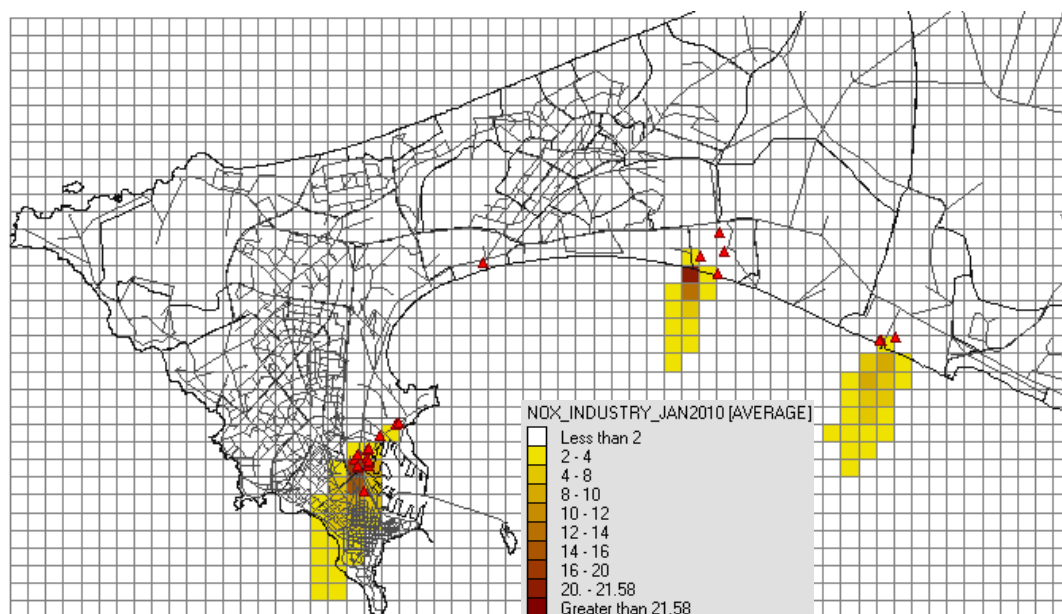


Figure 11: Average concentration of NO<sub>x</sub> for January 2010, modelled with emissions from industrial sources. The red triangles in the figures indicate the location of the industrial stacks.

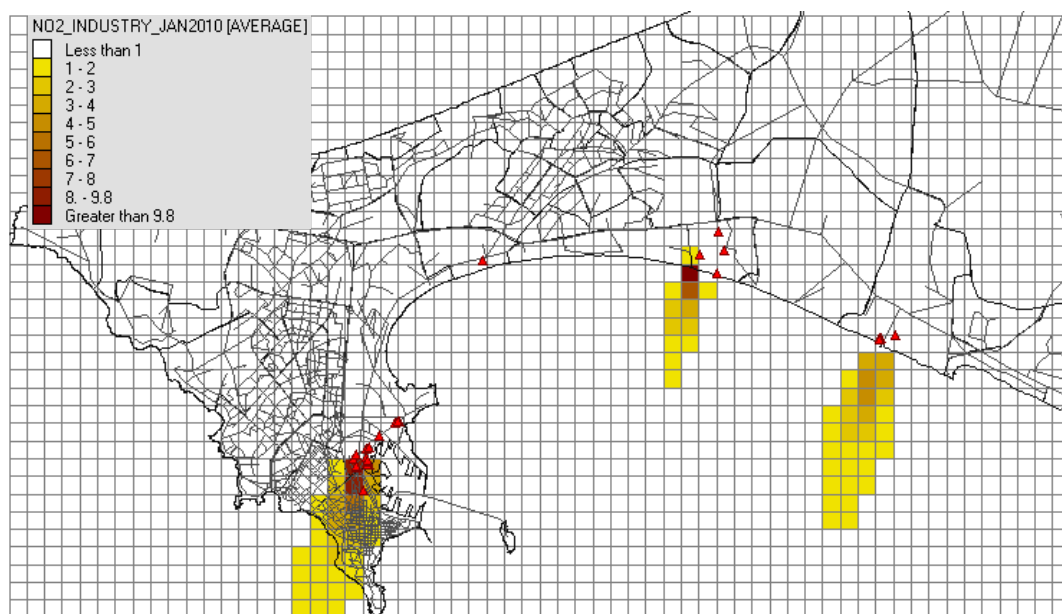


Figure 12: Average concentration of NO<sub>2</sub> for January 2010, modelled with emissions from industrial sources.

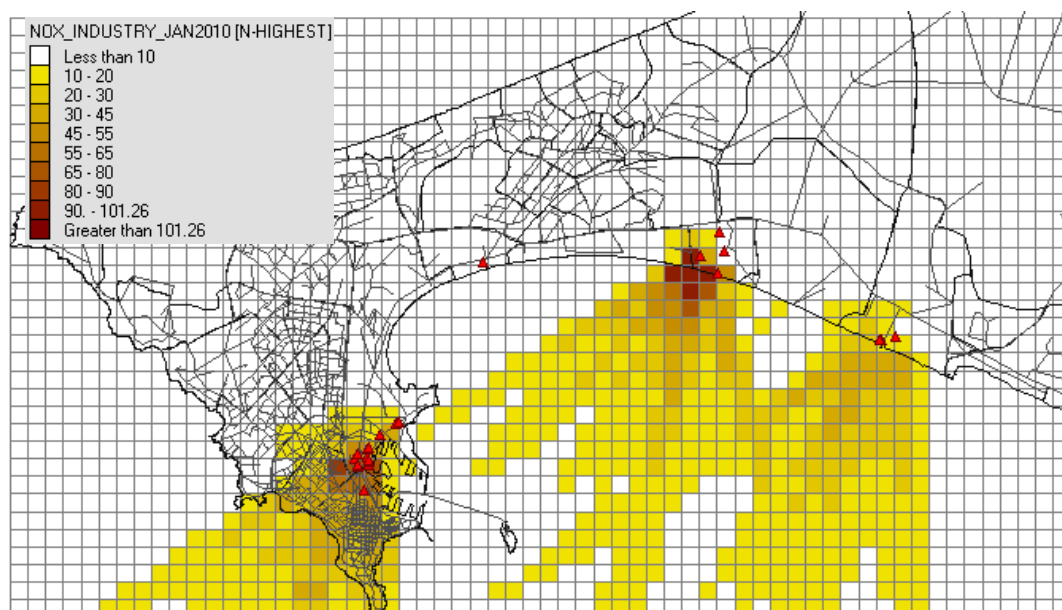


Figure 13: Maximum hourly concentration of NO<sub>x</sub> in January 2010, modelled with emissions from industrial sources.

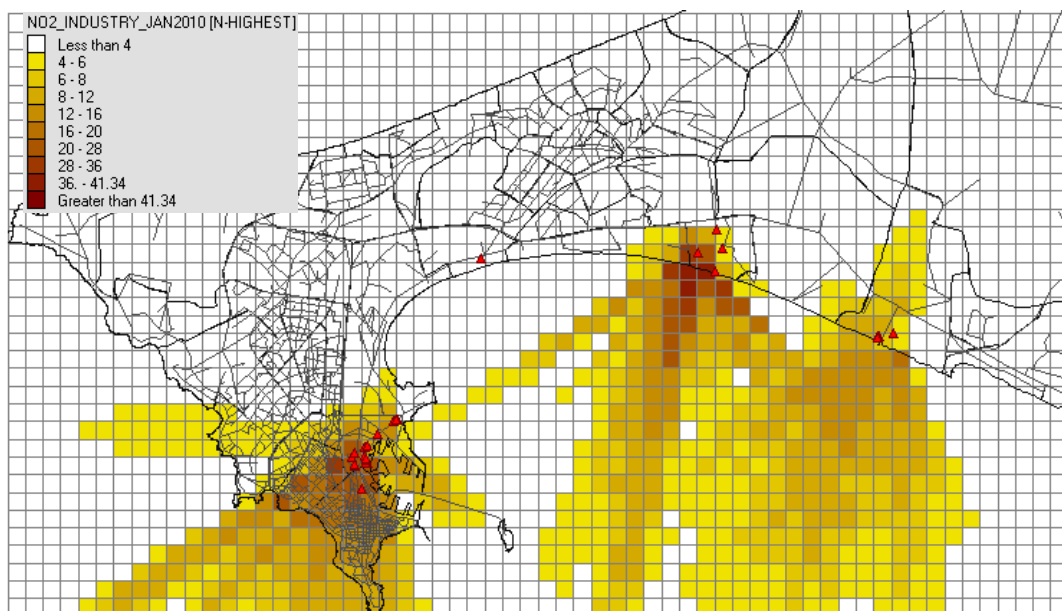


Figure 14: Maximum hourly concentration of NO<sub>2</sub> in January 2010, modelled with emissions from industrial sources.



#### 5.1.4 Contribution from traffic sources

The average concentration fields of NO<sub>x</sub> and NO<sub>2</sub> calculated with emissions from traffic sources included in the AirQUIS emission database (Guerreiro and Dam, 2010) are shown in Figure 15 and Figure 16, respectively. The maximum 500 x 500 m<sup>2</sup> average modelled concentration is 34 µg/m<sup>3</sup> for NO<sub>2</sub> and 83 µg/m<sup>3</sup> for NO<sub>x</sub>.

The hourly maximum concentration fields of NO<sub>x</sub> and NO<sub>2</sub> calculated with emissions from traffic sources, are shown in Figure 17 and Figure 18, respectively. The maximum 500 x 500 m<sup>2</sup> hourly concentration is 155 µg/m<sup>3</sup> for NO<sub>2</sub> and 843 µg/m<sup>3</sup> for NO<sub>x</sub>.

In average the traffic sources included in the emission database contribute to about 93% of the NO<sub>2</sub> concentrations calculated with the contribution from all sources. This is despite the fact that the traffic sources contribute to 67% of the total NO<sub>x</sub> emissions and to 82% of the primary NO<sub>2</sub> emissions (Table 5). As it was pointed out in previous chapters, industrial emission plumes get elevated in the air, due to the stack height, the exhaust gas temperature and velocity and disperses before meeting the ground. Traffic emissions are emitted at ground level, having a more direct impact on ground level concentrations.

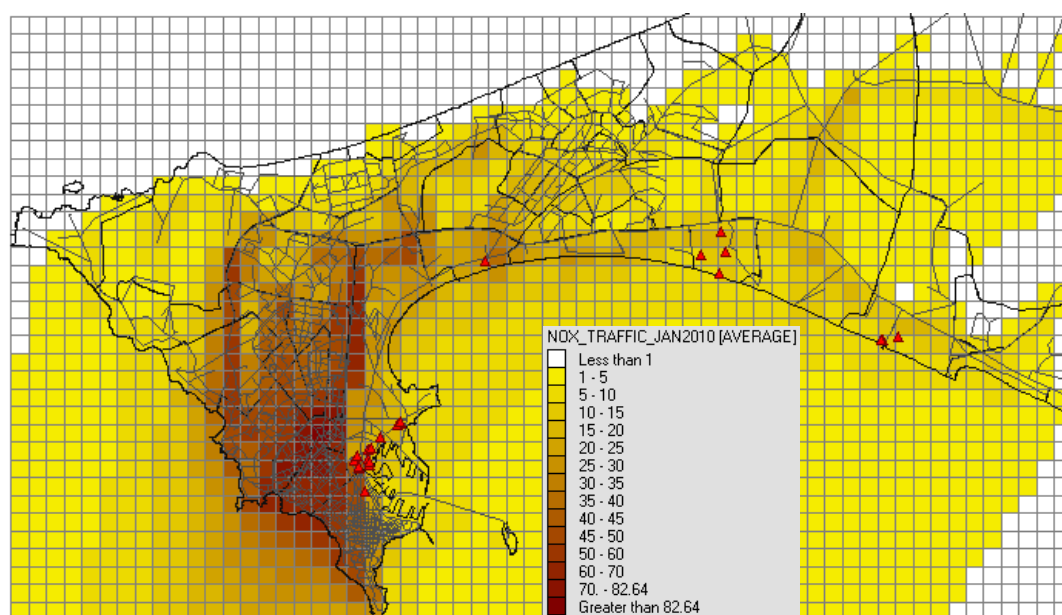


Figure 15: Average concentration of NO<sub>x</sub> for January 2010, modelled with emissions from traffic sources.

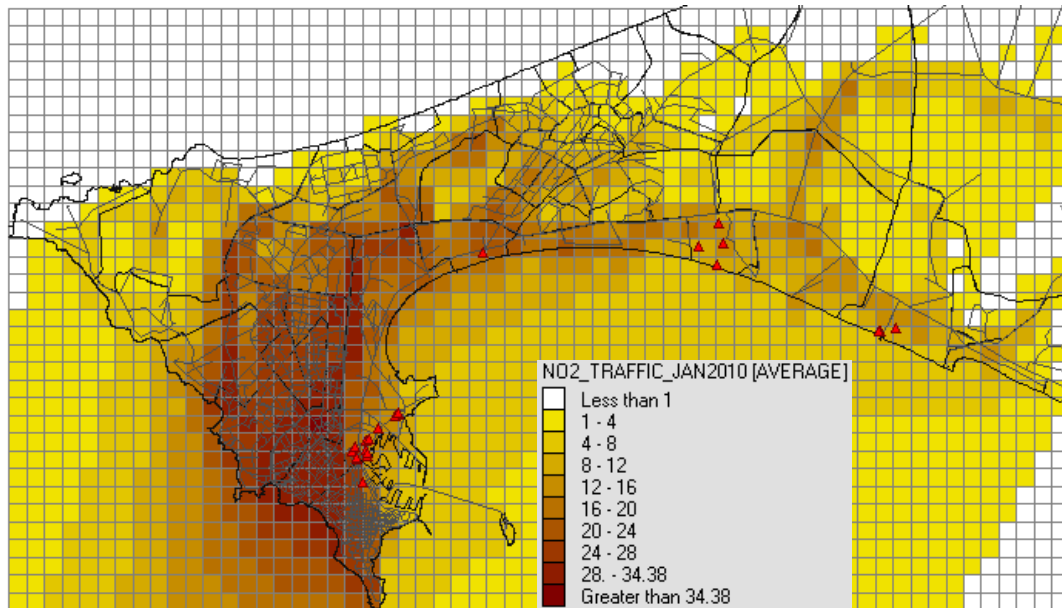


Figure 16: Average concentration of NO<sub>2</sub> for January 2010, modelled with emissions from traffic sources.

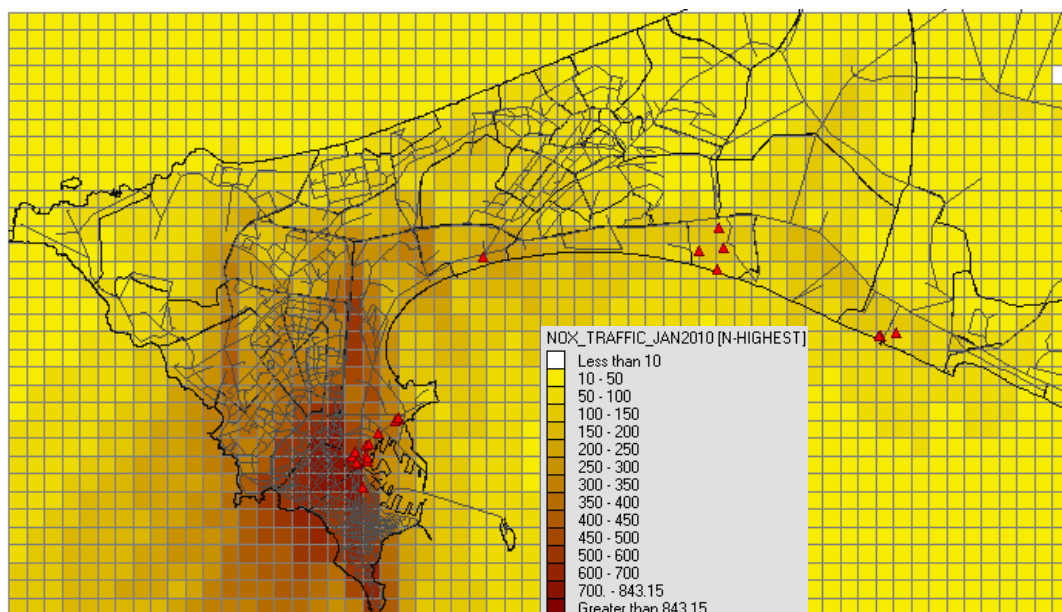


Figure 17: Maximum hourly concentration of NO<sub>x</sub> in January 2010, modelled with emissions from traffic sources.



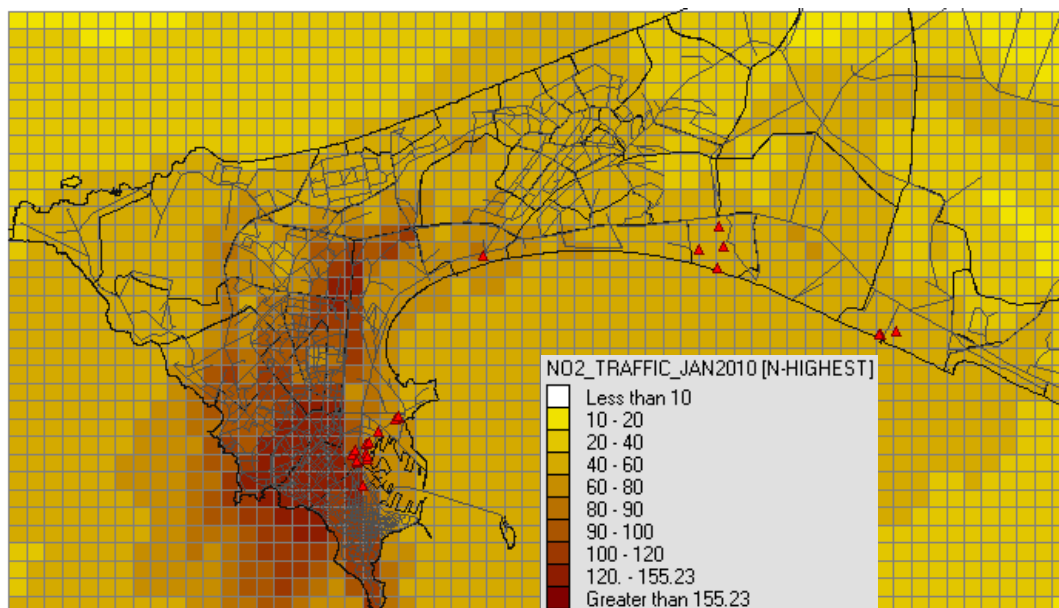


Figure 18: Maximum hourly concentration of NO<sub>2</sub> in January 2010, modelled with emissions from traffic sources.

### 5.1.5 Contribution from area sources

The average concentration fields of NO<sub>x</sub> and NO<sub>2</sub> calculated with emissions from area sources included in the AirQUIS emission database (Guerreiro and Dam, 2010) are shown in Figure 19 and Figure 20, respectively. The maximum 500 x 500 m<sup>2</sup> average modelled concentration is 1.85 µg/m<sup>3</sup> for NO<sub>2</sub> and 2.3 µg/m<sup>3</sup> for NO<sub>x</sub>.

The hourly maximum concentration fields of NO<sub>x</sub> and NO<sub>2</sub> calculated with emissions from traffic sources are shown in Figure 21 and Figure 22, respectively. The maximum 1 km<sup>2</sup> hourly concentration is 28.6 µg/m<sup>3</sup> for NO<sub>2</sub> and 34.3 µg/m<sup>3</sup> for NO<sub>x</sub>.

In average the area sources included in the emission database contribute to about 3% of the NO<sub>2</sub> concentrations calculated with the contribution from all sources. Area sources contribute to 1% of the total NO<sub>x</sub> and NO<sub>2</sub> emissions (Table 5). Area sources have a higher relative contribution to ground level concentrations than to the total emission, due to the fact they emit much closer to the ground (at about 3 to 4 meters height) than the industrial emissions.

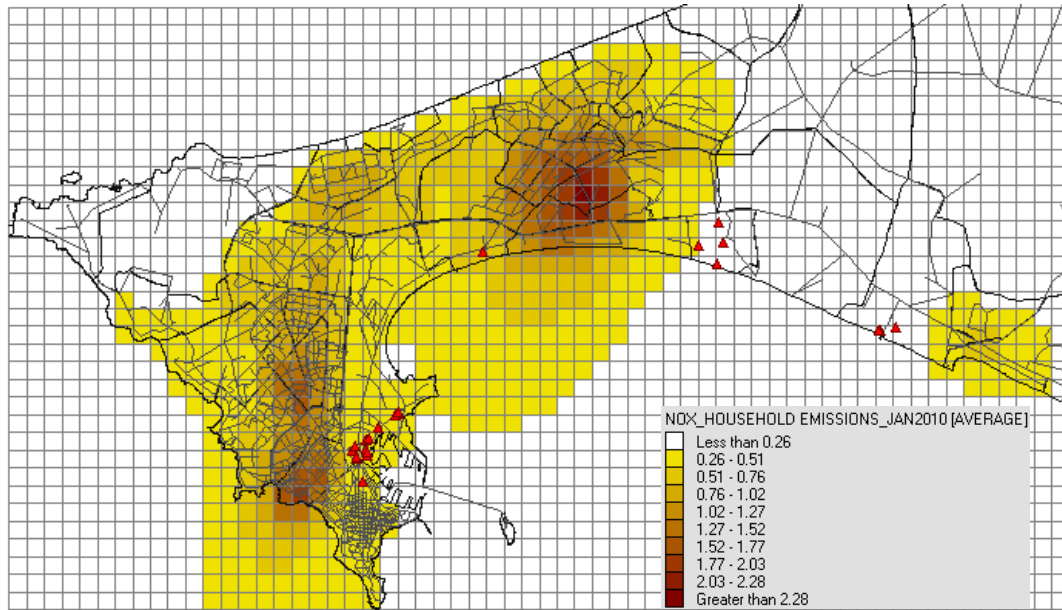


Figure 19: Average concentration of NO<sub>x</sub> for January 2010, modelled with emissions from area sources.

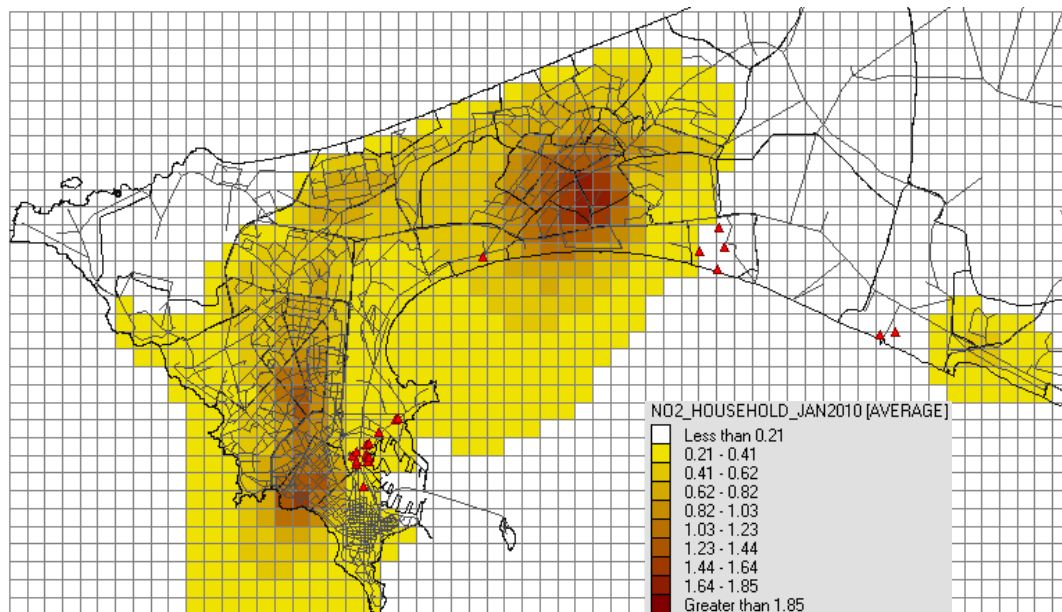


Figure 20: Average concentration of NO<sub>2</sub> for January 2010, modelled with emissions from area sources.

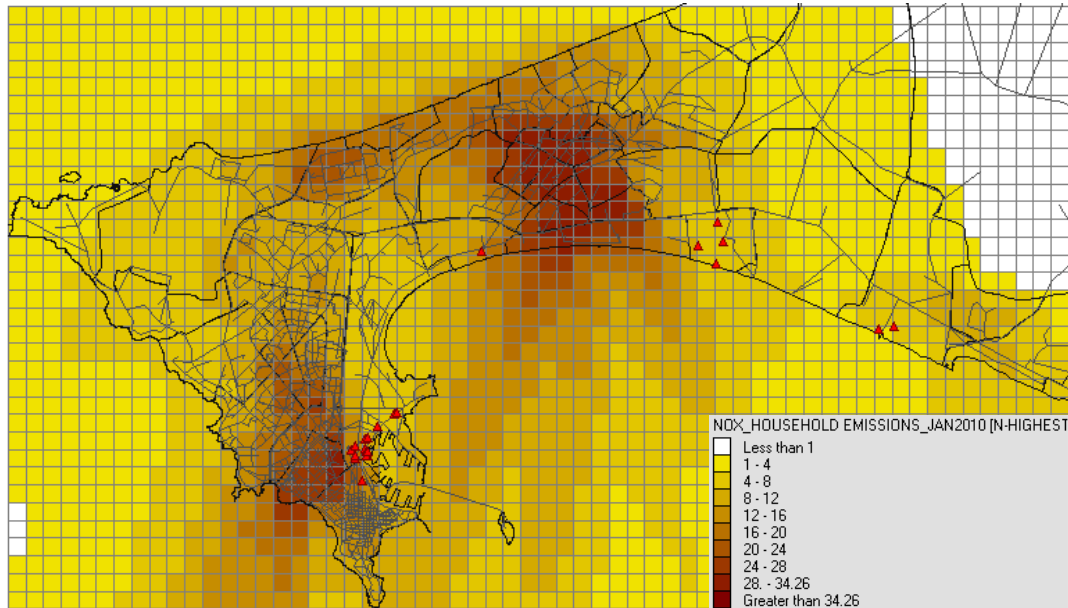


Figure 21: Maximum hourly concentration of NO<sub>x</sub> in January 2010, modelled with emissions from area sources.

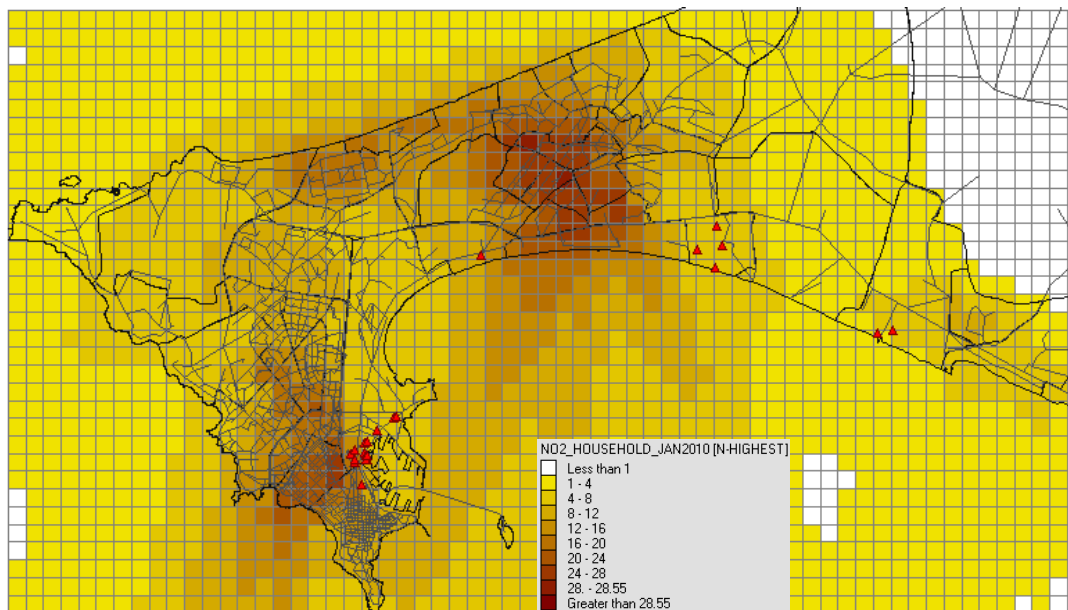


Figure 22: Maximum hourly concentration of NO<sub>2</sub> in January 2010, modelled with emissions from area sources.

### 5.1.6 Comparison of modelled and measured concentrations

A first attempt to compare modelled and measured concentrations is presented in this report. The short time series and quality of the measurement data do not allow us to perform a full comparison. However, the main objective of this exercise was to train the CGQA modelling expert in the interpretation of model results, analysing concentrations in relation to meteorological conditions, understand the assumptions and limitations of the models and of the emission inventory.

Figure 23 shows one week time series of hourly values of modelled and measured NO<sub>2</sub> concentrations at the Bel Air station, and Table 6 shows the descriptive statistics of modelled and measured NO<sub>2</sub> hourly concentrations for the month of January.

As one can see both from the figure and from the minimum values in the table, the NO<sub>2</sub> regional background concentration of 4 µg/m<sup>3</sup> should be added to the modelled concentrations, in order to account for the NO<sub>2</sub> concentration transported from outside the model domain. This correction would minor the gap between the modelled and measured night concentrations.

When comparing hourly modelled concentrations to measured concentrations, one considers the modelled result as acceptable when the modelled concentrations are within 50% to 200% of the measured concentration value. The comparison is quite good considering that this is a first test of the model and that the emission characterisation is not updated for 2010. The hourly variation of the traffic flow is easily seen both on the measured and modelled concentrations and both the mean and minimum concentrations are very close, when the background concentration is taken into account, as shown in Table 6.

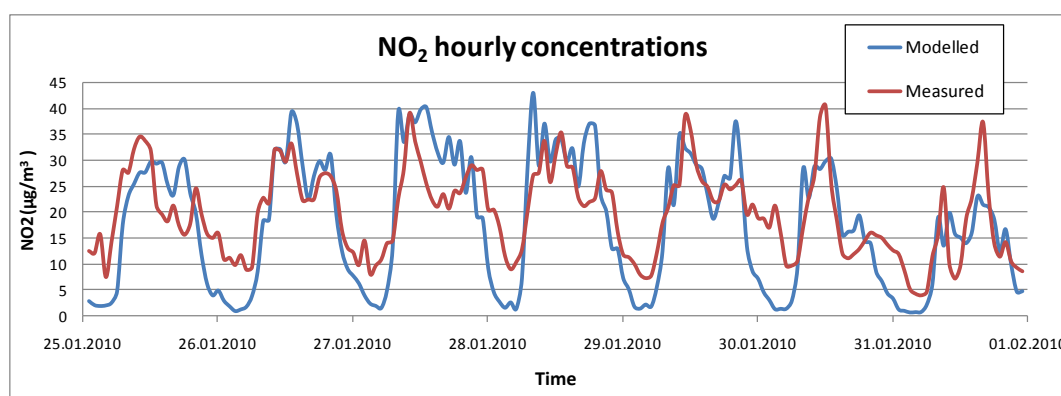


Figure 23: Comparison of hourly concentrations of NO<sub>2</sub> (January 2010) measured at the Bel Air monitoring station and modelled at the same station location.

Table 6: Descriptive statistics of measured and modelled NO<sub>2</sub> and NO<sub>x</sub> hourly concentrations for January 2010 at the Bel Air station.

	NO <sub>2</sub> (µg/m <sup>3</sup> )			NO <sub>x</sub> (µg/m <sup>3</sup> )		
	Modelled	Modelled + back. Conc.	Measured	Modelled	Modelled + back. Conc.	Measured
<b>Maximum</b>	80	84	54	390	396	381
<b>Minimum</b>	0	4	4	1	7	10
<b>Average</b>	16	20	21	50	57	67

## 5.2 SO<sub>2</sub> concentrations

### 5.2.1 Background concentrations

In order to simplify the interpretation of the modelled concentration results and the contribution from the different source types to the ambient air concentrations, a SO<sub>2</sub> background concentration of 0 µg/m<sup>3</sup> was assumed. The average background concentration of SO<sub>2</sub> is about 3 µg/m<sup>3</sup> (Sivertsen et al, 2006).

### 5.2.2 Contribution from all sources

The average concentration field of SO<sub>2</sub> calculated based on emissions from all sources is shown in Figure 24. The maximum 500 x 500 m<sup>2</sup> average modelled SO<sub>2</sub> concentration is 56 µg/m<sup>3</sup>. In order to account for the SO<sub>2</sub> concentration transported from outside the model domain, the regional background concentration of SO<sub>2</sub> of 3 µg/m<sup>3</sup> (see Chapter 5.2.1) should be added to the modelled concentrations, leading to an average SO<sub>2</sub> concentration of 59 µg/m<sup>3</sup>. This is a high concentration of SO<sub>2</sub>, which is above the Senegalese limit value for yearly average of SO<sub>2</sub> (i.e. 50 µg/m<sup>3</sup>). However, we are comparing a month average with an annual average limit value, which is an acceptable approximation if the January 2010 average is representative for the year.

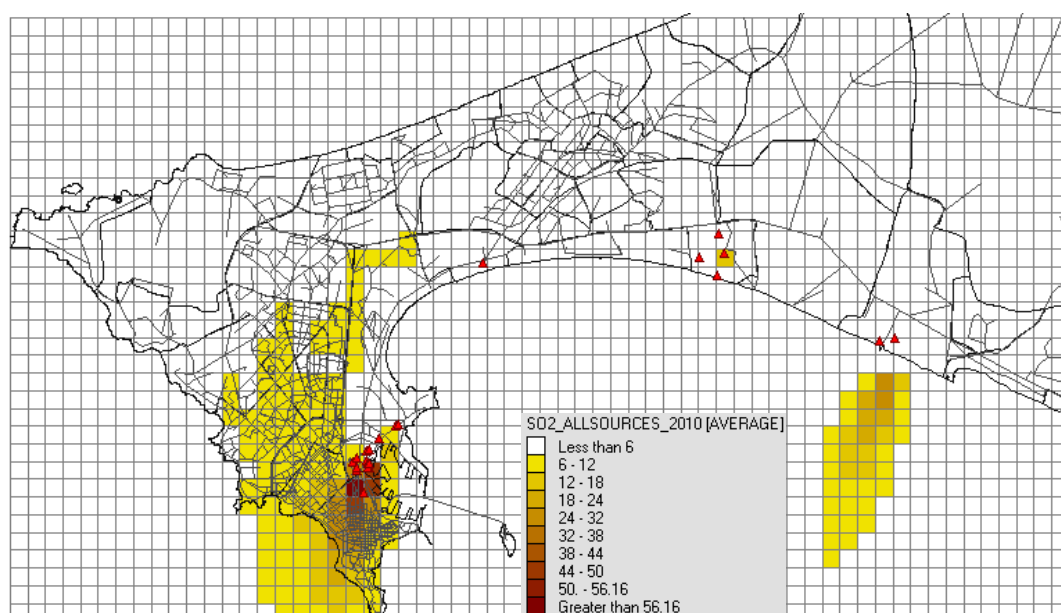


Figure 24: Average concentration of SO<sub>2</sub> for January 2010, modelled with emissions from all sources. The red triangles in the figures indicate the location of the industrial stacks.

### 5.2.3 Contribution from industrial sources

The average concentration field of SO<sub>2</sub> calculated with emissions from industrial sources included in the AirQUIS emission database (Guerreiro and Dam, 2010) is shown in Figure 25. The industrial sources included in the emission database contribute to about 35% of the SO<sub>2</sub> concentrations calculated with the contribution from all sources. This is despite the fact that the industrial sources contribute to 90% of the total SO<sub>2</sub> emissions (Table 5). The reason for this is that the industrial emissions are emitted through stacks, up to 76 meters high, as explained in the previous chapters.

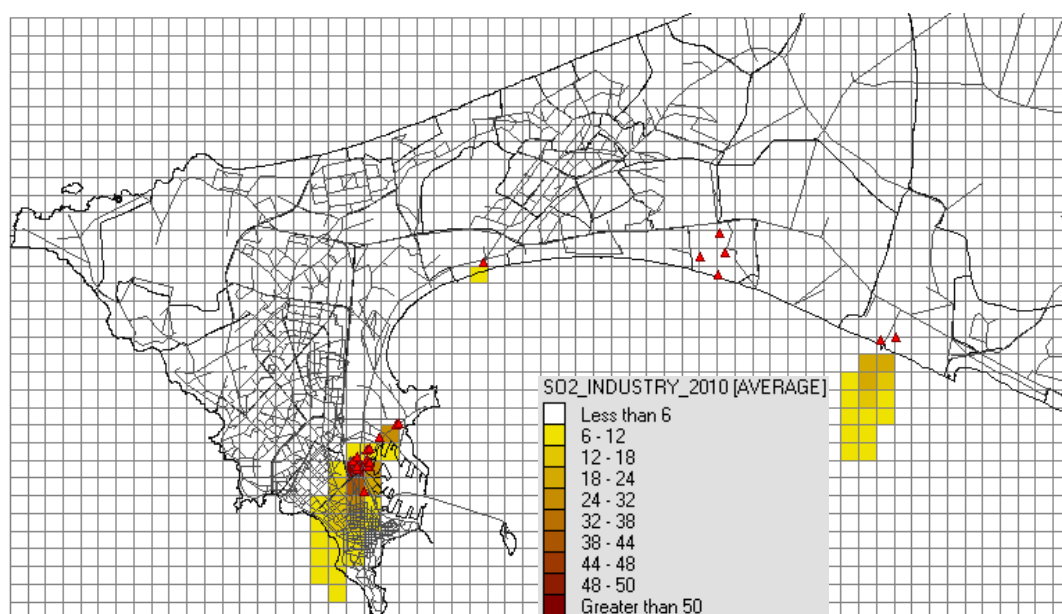


Figure 25: Average concentration of SO<sub>2</sub> for January 2010 modelled with emissions from industrial sources.



#### 5.2.4 Contribution from traffic sources

The average concentration field of SO<sub>2</sub> calculated with emissions from industrial sources included in the AirQUIS emission database (Guerreiro and Dam, 2010) is shown in Figure 26. The maximum 500 x 500 m<sup>2</sup> average modelled SO<sub>2</sub> concentration is 9 µg/m<sup>3</sup>.

In average the traffic sources included in the emission database contribute to about 54% of the SO<sub>2</sub> concentrations calculated with the contribution from all sources. This is despite the fact that the traffic sources only contribute to 9% of the total SO<sub>2</sub> emissions (Table 5). As explained earlier, this is due to the fact that the industrial emissions are emitted through high stacks, while traffic and area sources emissions are emitted at ground level, having a direct impact on ground level concentrations.

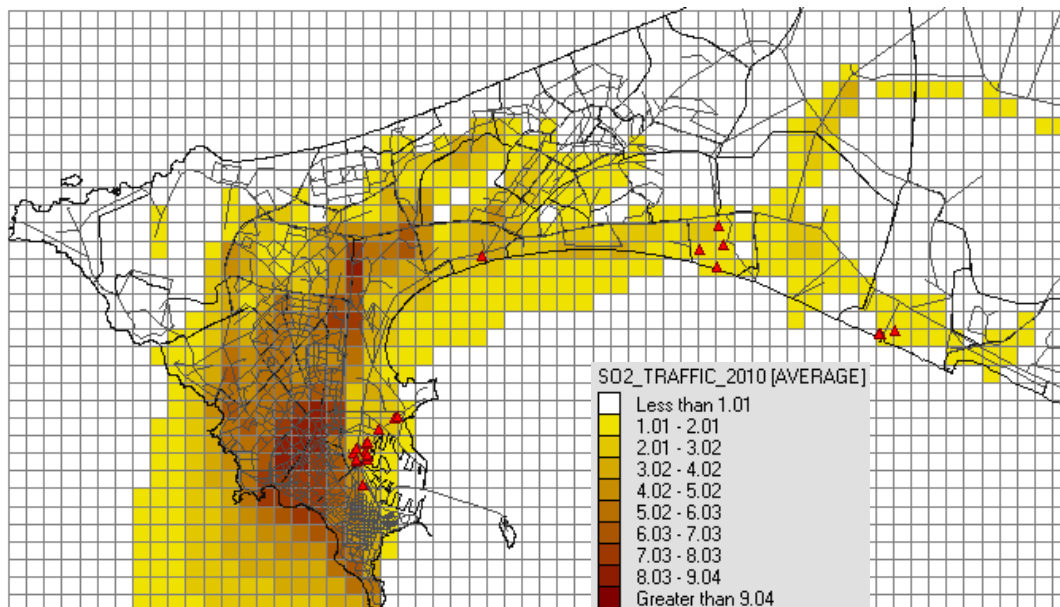


Figure 26: Average concentration of SO<sub>2</sub> for January 2010, modelled with emissions from traffic sources.



### 5.2.5 Contribution from area sources

The average concentration field of SO<sub>2</sub> calculated with emissions from industrial sources is shown in Figure 27. The maximum 500 x 500 m<sup>2</sup> average modelled SO<sub>2</sub> concentration is 2 µg/m<sup>3</sup>.

In average the area sources included in the emission database contribute to about 11% of the SO<sub>2</sub> concentrations calculated with the contribution from all sources. Area sources contribute to only 1% of the total SO<sub>2</sub> emissions (Table 5). Area sources have a higher relative contribution to ground level concentrations than to the total emission, due to the fact they emit much closer to the ground (at about 3 to 4 meters height) than the industrial emissions.

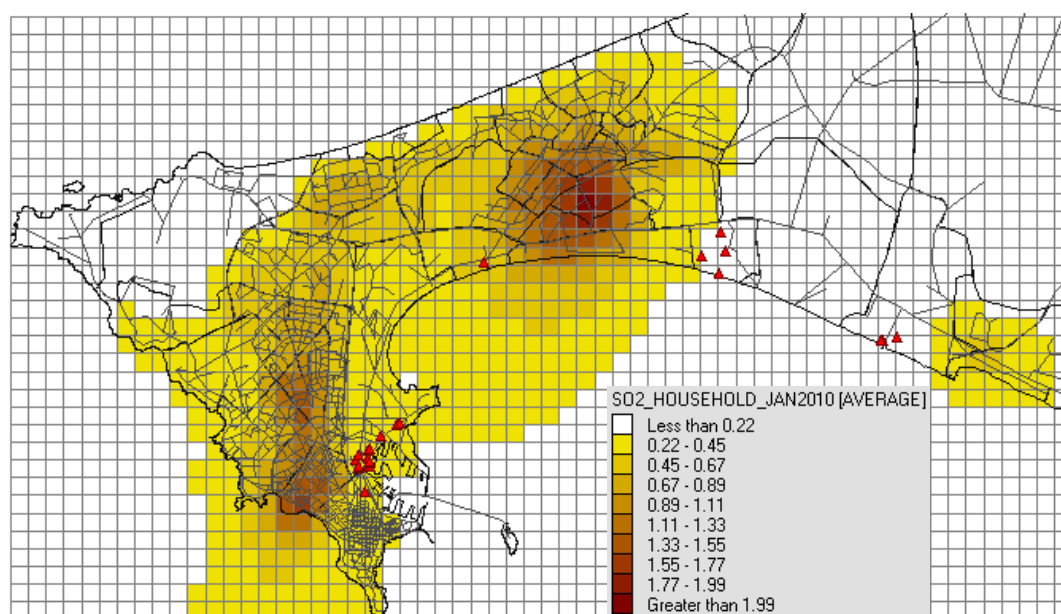


Figure 27: Average concentration of SO<sub>2</sub> for January 2010, modelled with emissions from area sources.

### 5.2.6 Comparison of modelled and measured concentrations

A first attempt to compare modelled and measured SO<sub>2</sub> concentrations is presented here. Figure 28 shows one week time series of hourly values of modelled and measured SO<sub>2</sub> concentrations at the Bel Air station, and Table 7 shows the descriptive statistics of modelled and measured SO<sub>2</sub> hourly concentrations for January 2010.

The SO<sub>2</sub> regional background concentration of 3 µg/m<sup>3</sup> should be added to the modelled concentrations, in order to account for the SO<sub>2</sub> concentration transported from outside the model domain. This correction minors the gap between the modelled and measured night concentrations.

The hourly variation of the traffic flow is easily seen both on the measured and modelled concentrations. The model predicts higher peak concentrations in day

time. This station is influenced by the relatively important industrial emissions from stacks. It is often difficult to model correctly hourly concentrations from stacks and specially the peaks. The mean, maximum and minimum concentrations are comparable when the background concentration is taken into account (Table 7). For air pollution dispersion models, a modelled hourly concentration within 50% to 200% of the measured concentration is a good result.

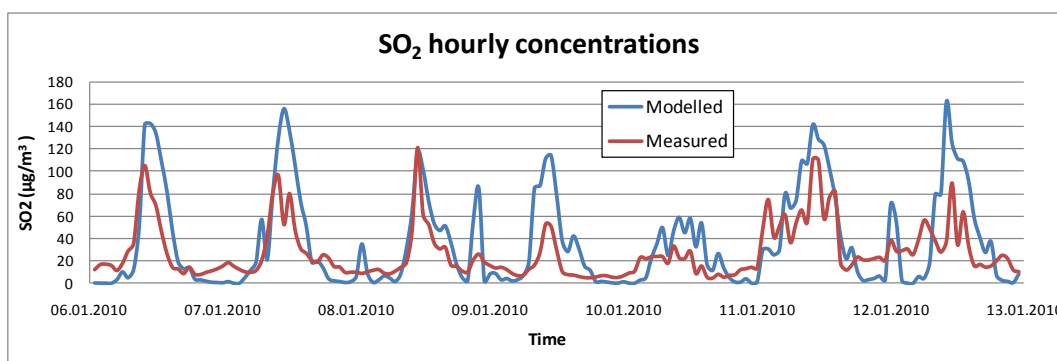


Figure 28: Comparison of hourly concentrations of SO<sub>2</sub> (January 2010) measured at the Bel Air monitoring station and modelled at the same station location.

Table 7: Descriptive statistics of measured and modelled SO<sub>2</sub> hourly concentrations for January 2010 at Bel Air station.

	SO <sub>2</sub> (µg/m <sup>3</sup> )		
	Modelled	Modelled + back. Conc.	Measured
<b>Maximum</b>	186	189	150
<b>Minimum</b>	0	3	3
<b>Average</b>	33	36	22

### 5.3 CO concentrations

The contribution from industrial sources to CO concentrations is not shown in this chapter, as there is only information on CO emissions from two industries, which is not enough to justify the dispersion calculation and to obtain representative results.

#### 5.3.1 Background concentrations

In order to simplify the interpretation of the modelled concentration results and the contribution from the different source types to the ambient air concentrations, a CO background concentration of  $0 \mu\text{g}/\text{m}^3$  was assumed, which is a correct assumption for CO concentrations.

#### 5.3.2 Contribution from traffic and area sources

The average concentration field of CO calculated with emissions from traffic and area sources is shown in

Figure 29. The maximum  $500 \times 500 \text{ m}^2$  average modelled CO concentration is  $2\,004 \mu\text{g}/\text{m}^3$ .

The hourly maximum concentration field of CO calculated with emissions from traffic and area sources is shown in Figure 30. The maximum calculated  $500 \times 500 \text{ m}^2$  CO hourly concentration is about  $29\,200 \mu\text{g}/\text{m}^3$ , which is very high compared to the Senegalese limit value for hourly CO concentration (i.e.  $30\,000 \mu\text{g}/\text{m}^3$ ; Table 2).

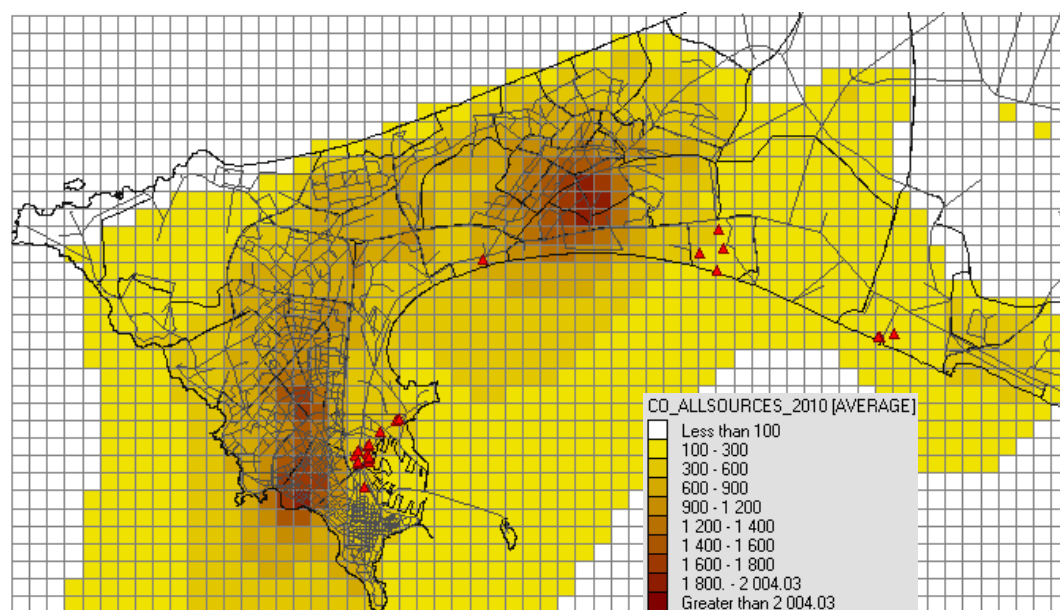


Figure 29: Average concentration of CO for January 2010, modelled with emissions from traffic and area sources.

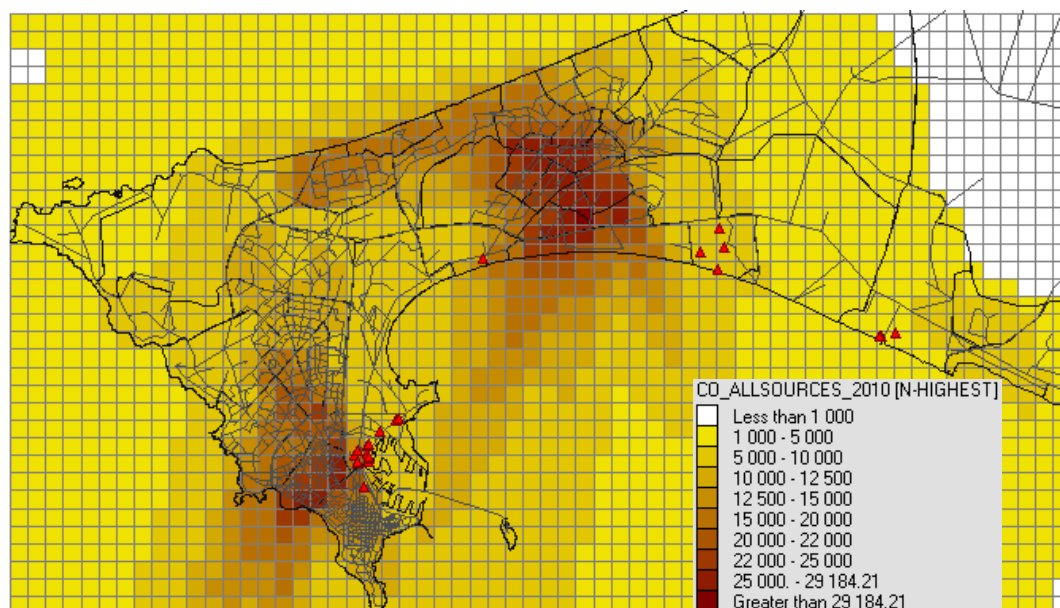


Figure 30: Maximum hourly concentration of CO in January 2010, modelled with emissions from traffic and area sources.

Note that to calculate the hourly maximum concentration field, the model chooses the hour with the highest calculated concentration within the modelled period (January 2010) for each grid cell, and attributes it to the grid cell as the maximum hourly concentration.

### 5.3.3 Contribution from traffic sources

The average concentration field of CO calculated with emissions from traffic sources is shown in Figure 31. The maximum  $500 \times 500 \text{ m}^2$  average modelled CO concentration is  $522 \mu\text{g}/\text{m}^3$ .

The hourly maximum concentration field of CO is shown in Figure 32. The maximum calculated  $500 \times 500 \text{ m}^2$  CO hourly concentration is about  $5\,000 \mu\text{g}/\text{m}^3$ , which is quite high considering that the modelled results presented here represent concentrations averaged within a grid cell of  $500 \times 500 \text{ m}^2$ , and the concentrations of CO near the road side may be even higher.

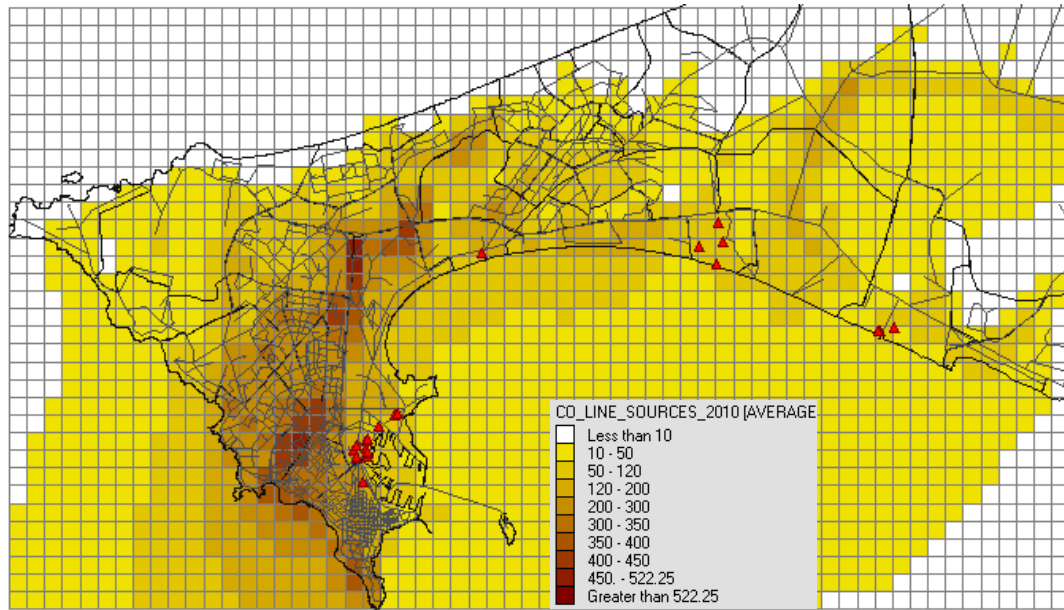


Figure 31: Average concentration of CO for January 2010 modelled with emissions from traffic sources.

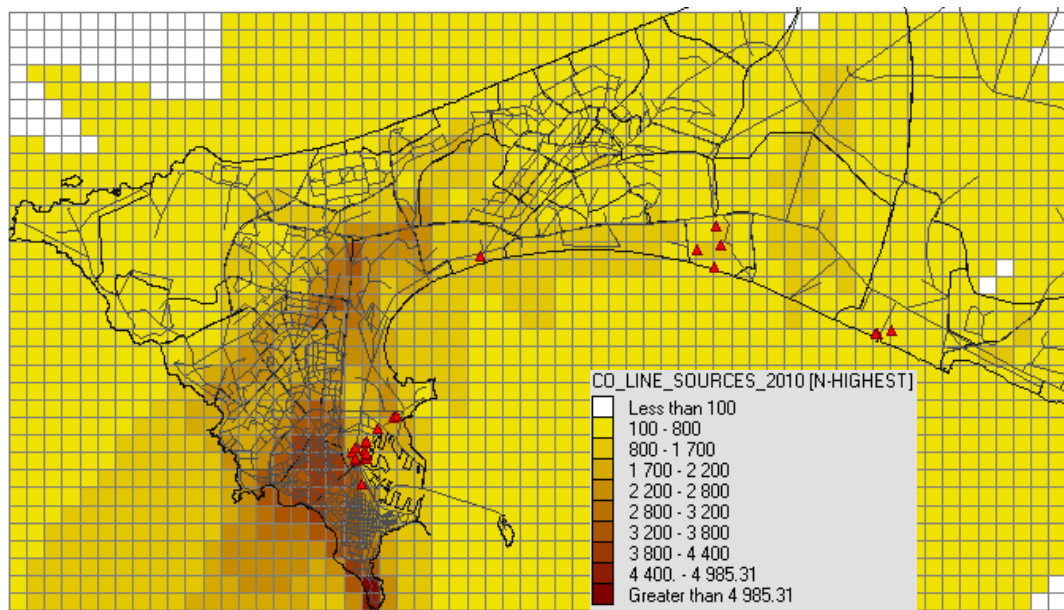


Figure 32: Maximum hourly concentration of CO in January 2010 modelled with emissions from traffic sources.

### 5.3.4 Contribution from area sources

The average concentration field of CO calculated with emissions from area sources is shown in Figure 33. The maximum 500 x 500 m<sup>2</sup> average modelled CO concentration is 1.923 µg/m<sup>3</sup>.

The hourly maximum concentration field of CO is shown in Figure 34. The maximum hourly CO concentration calculated on 1 km<sup>2</sup> is about 28.900 µg/m<sup>3</sup>, which is almost the Senegalese limit value for hourly CO concentration (i.e. 30.000 µg/m<sup>3</sup>; Table 2).

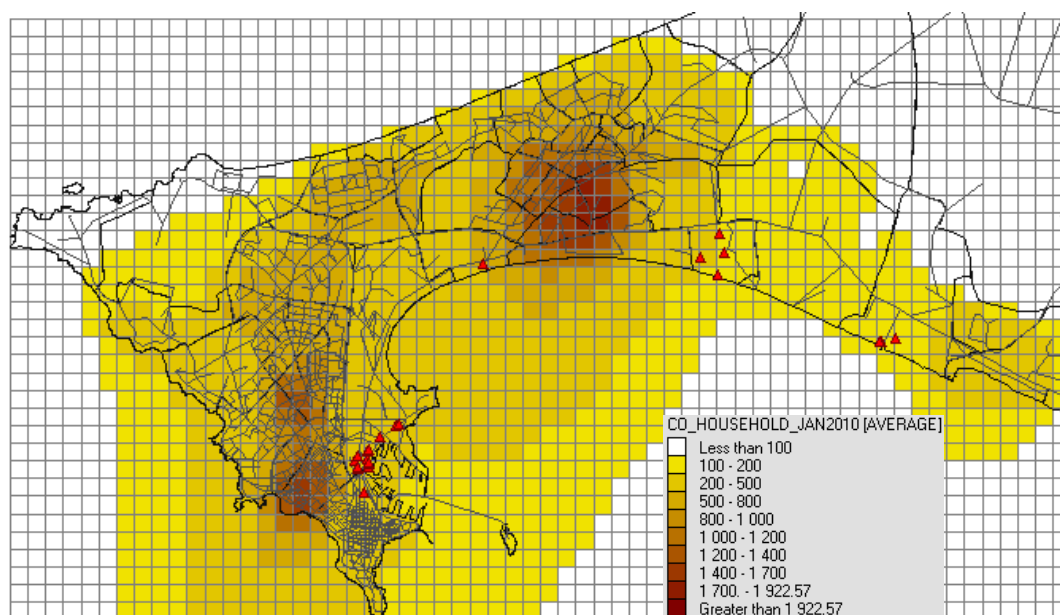


Figure 33: Average concentration of CO for January 2010 modelled with emissions from area sources.

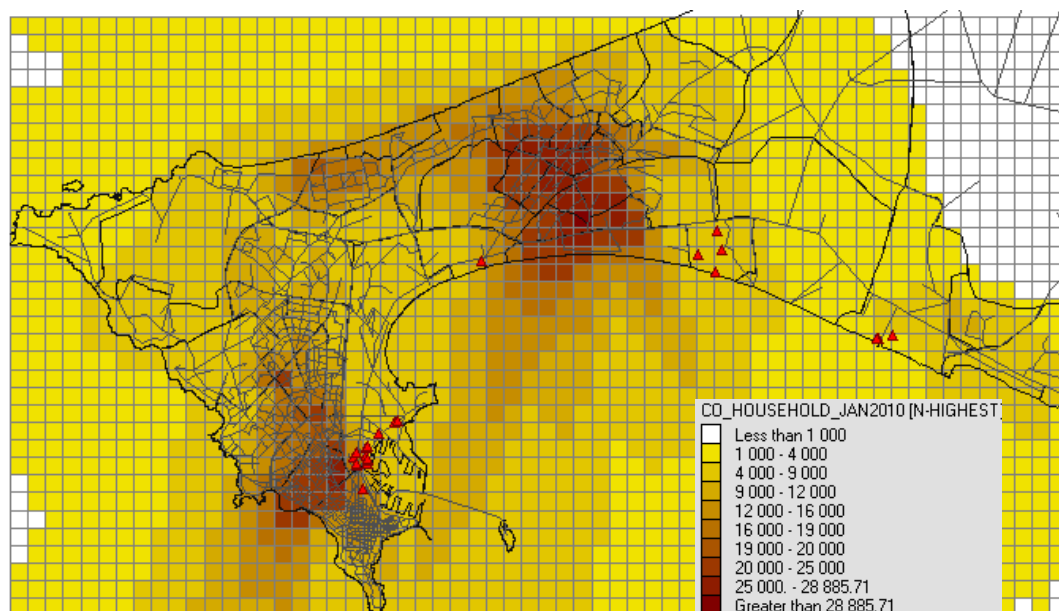


Figure 34: Maximum hourly concentration of CO in January 2010 modelled with emissions from area sources.

### 5.3.5 Comparison of model results and measurements

Figure 35 shows one week time series of hourly values of modelled and measured CO concentrations at the Medina station and Table 8 shows the descriptive statistics of modelled and measured CO hourly concentrations for January, 2010.

At this location, the dominant source of CO is traffic. This can be seen in the measured and modelled hourly concentrations, as the hourly variation of the traffic flow is easily seen both on the measured and modelled concentrations. The maximum and minimum concentrations are comparable, but the modelled average concentration is over two times higher than the measured concentration (Table 7). The model might overestimate to a certain extent the CO concentrations. But we cannot exclude the possibility that the CO monitor measured lower concentrations during this month.

Table 8: Descriptive statistics of measured and modelled CO hourly concentrations for January 2010 at Medina station.

	CO ( $\mu\text{g}/\text{m}^3$ )	
	Modelled	Measured
<b>Maximum</b>	433	412
<b>Minimum</b>	11	1
<b>Average</b>	4027	1470



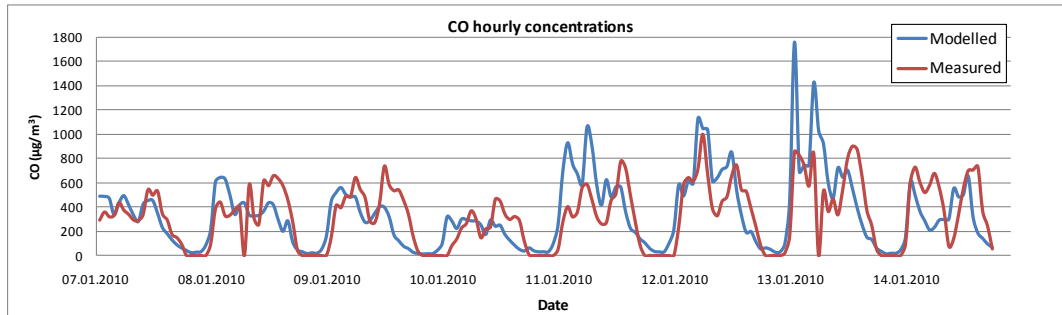


Figure 35: Comparison of hourly concentrations of CO in January 2010 measured at the Medina monitoring station and modelled at the station location.



## 6 Conclusion

The amount of air quality measurement data available at the end of the project was neither adequate nor sufficient to fully test the AirQUIS dispersion model in Dakar. Therefore only a preliminary evaluation of the AirQUIS models and air quality modelling for Dakar was possible to undertake. The current report summarised the preliminary results from air quality modelling in Dakar.

The results showed that the industrial sources have a lower impact on ground level concentrations of SO<sub>2</sub> and NO<sub>2</sub> than traffic and area sources, even if they have a relatively high share of the total emissions, being responsible for 90% of the total SO<sub>2</sub> emissions in the inventory and for 32% of the NO<sub>x</sub> emissions. Traffic is responsible for 93% of the modelled average NO<sub>2</sub> concentrations, while the 15 industries included in the database are responsible for 4% and household emissions for 3%. Concerning SO<sub>2</sub> average concentrations, the industries are responsible for 35%, traffic for 54% and households for 11%. The household emissions are responsible for 66% of the modelled CO average concentrations, while traffic is responsible for the remaining 34%. Industrial emissions were not included in the CO concentration calculations due to insufficient emission data.

The preliminary evaluation of the model shows satisfactory results, but a comparison of modelled and measured concentrations should be done for a whole year of data, in order to check all meteorological conditions and have a more solid statistical basis for the evaluation of the model.

## 7 References

- Denby, B. (2008) AirQUIS Module de Modélisation - Guide de l'utilisateur. Kjeller (NILU OR 23/2008).
- Foster, F., Walker, H., Duckworth, G., Taylor, A. and Sugiyama, G. (1995) User's guide to the CG-Mathew/Adpic models, Version 3.0. Livermore, CA, Lawrence Livermore National Laboratory (Report UCRL-MA-103581 Rev. 3).
- Guerreiro C. And Dam, V.T. (2010) A bottom-up air pollution emission inventory for Dakar. Kjeller (NILU OR 53/2010).
- ASN (2003) Pollution atmosphérique - Norme de rejets, Direction de l'Environnement et des Etablissements classés. Octobre 2003. Dakar, Association Sénégalaise de Normalisation (Norme Sénégalaise NS 05-062).
- Sivertsen, B., Laupsa, H. et Guerreiro, C. (2006) Etude d'évaluation de l'état de la pollution de l'air à Dakar 2005. Octobre - décembre 2005 et janvier 2006. Kjeller (NILU OR 58/2006).
- Sivertsen, B., Guerreiro, C. and Ly, I. (2010a) Air quality standards for Senegal. Kjeller (NILU OR 49/2010).
- Sivertsen, B., Ndiaye, A. and Diop, M. (2010b) Air Quality Monitoring in Dakar - Monthly Report N° 01/2010. Kjeller (NILU OR 19/2010).
- Sherman, C.A. (1978). A mass consistent model for wind fields over complex terrain. *J. Appl. Meteorol.*, 17, 312-319.
- Slørdal, L.H. (2001) Application of MATHEW in AirQUIS/Episode. Revision of the export routine. Kjeller (NILU TR 3/2001) (In Norwegian).
- Slørdal, L.H. (2002). MATHEW as applied in the AirQUIS System. Model description. Kjeller (NILU TR 9/2002).
- Slørdal, L.H., Walker, S.E. and Solberg, S. (2003) The urban air dispersion model EPISODE applied in AirQUIS 2003. Technical description. Kjeller (NILU TR 12/2003).
- WHO (2000) Air quality guidelines for Europe, second edition. Copenhagen, WHO, Regional Office for Europe (WHO Regional Publications, European Series, No. 91). URL : <http://www.euro.who.int/document/e71922.pdf>
- WHO (2005) Air quality guidelines, Global update 2005. Particulate matter, ozone, nitrogen dioxide and sulfur dioxide. Copenhagen, WHO, Regional Office for Europe. URL: [http://www.euro.who.int/\\_data/assets/pdf\\_file/0005/78638/E90038.pdf](http://www.euro.who.int/_data/assets/pdf_file/0005/78638/E90038.pdf)





REFERENCE: O-105010 OR 52/2010  
DATE: JULY 2010  
ISBN: 978-82-425-2265-8 (Print)  
978-82-425-2266-5 (Electronic)

NILU is an independent, non-profit institution established in 1969. Through its research NILU increases the understanding of climate change, of the composition of the atmosphere, of air quality and of hazardous substances. Based on its research, NILU markets integrated services and products within analyzing, monitoring and consulting. NILU is concerned with increasing public awareness about climate change and environmental pollution.

REFERENCE: O-105010 OR 52/2010  
DATE: JULY 2010  
ISBN: 978-82-425-2265-8 (Print)  
978-82-425-2266-5 (Electronic)

NILU is an independent, non-profit institution established in 1969. Through its research NILU increases the understanding of climate change, of the composition of the atmosphere, of air quality and of hazardous substances. Based on its research, NILU markets integrated services and products within analyzing, monitoring and consulting. NILU is concerned with increasing public awareness about climate change and environmental pollution.

